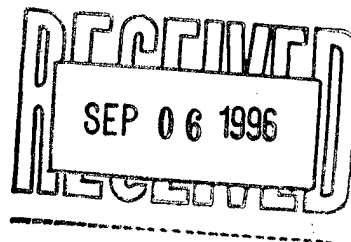


DOE/OR/00033--T742



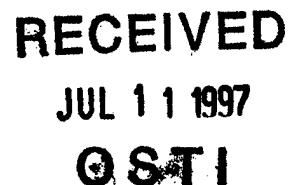
NEUTRON DOSIMETRY USING AQUEOUS SOLUTIONS
OF LITHIUM ACETATE

A Thesis

Presented in Partial Fulfillment of the Requirements for
the Degree Masters of Science in the
Graduate School of The Ohio State University

By

Lance John Rakovan, B.S.E.P.



The Ohio State University
1996

Master's Examination Committee:

Dr. Thomas E. Blue, Adviser

Dr. Nilendu Gupta

Approved by

Adviser

Nuclear Engineering Graduate Program

19980416 024

DISTRIBUTION OF THIS DOCUMENT IS UNLIMITED

MASTER

DISCLAIMER

This report was prepared as an account of work sponsored by an agency of the United States Government. Neither the United States Government nor any agency thereof, nor any of their employees, makes any warranty, express or implied, or assumes any legal liability or responsibility for the accuracy, completeness, or usefulness of any information, apparatus, product, or process disclosed, or represents that its use would not infringe privately owned rights. Reference herein to any specific commercial product, process, or service by trade name, trademark, manufacturer, or otherwise does not necessarily constitute or imply its endorsement, recommendation, or favoring by the United States Government or any agency thereof. The views and opinions of authors expressed herein do not necessarily state or reflect those of the United States Government or any agency thereof.

ABSTRACT

A thermal neutron dosimetry system using the ${}^6\text{Li}(n,\alpha){}^3\text{H}$ reaction and liquid scintillation counting of tritium was developed. Lithium acetate was chosen to supply the ${}^6\text{Li}$ in the aqueous dosimetry solutions. Neutron irradiations were completed using The Ohio State University Research Reactor. After two sets of samples were irradiated, variables in the system such as the mass of lithium acetate in the solutions and the counting window of the liquid scintillation counter used to analyze the sample were chosen. The system was evaluated by completing two sets of 23 minute irradiations with the reactor at 500 kW, 50 kW, 5 kW, and one irradiation at 500 W. The samples irradiated at 500 W were below the threshold of the system, and could not be used. Prompt analysis was essential due to loss of detectable emissions in the dosimetry solutions over time. The thermal neutron fluences calculated with the data from the samples were compared to the fluences determined from gold wire irradiations. The fluence values differed at most by 6%. The fluence values calculated from the samples were consistently less than those determined from the gold wires.

To My Parents and Family
&
In Memory of Frank, Sally, John,
And Jean

ACKNOWLEDGMENTS

I would like to thank a number of individuals for their aid in completing this project. I would like to express my thanks to Mr. Kevin Herminghuysen and Mr. Rick Myser, who donated much time and advice; Mr. Albert Vest and the Office of Environmental Health and Safety for the use of their liquid scintillation counter; Dr. Nilendu Gupta for the time and effort he put in as a member of my graduate studies committee; and my fellow students in The Ohio State University Nuclear Engineering Program for their input and aid.

The research was performed under appointment to the Applied Health Physics Fellowship Program administered by Oak Ridge Institute for Science and Education under contract number DE-AC05-76OR00033 between the U.S. Department of Energy and Oak Ridge Associated Universities. I am grateful to Mr. Tom Richmond, the program manager, and Ms. Rose Etta Cox for all of their assistance and support over the last two years.

I would especially like to express my gratitude to Dr. Thomas Blue for his support, guidance, and patience in the past few years.



1993 B.S. Engineering Physics,
The Ohio State University.

Sept. 1993 - Aug. 1994 Graduate Research Assistant,
Nuclear Engineering Program,
The Ohio State University.

Sept. 1994 - present DOE Applied Health Physics Fellow
Nuclear Engineering Program,
The Ohio State University.

FIELDS OF STUDY

Major Field: Nuclear Engineering

Studies in health physics and medical physics.

TABLE OF CONTENTS

ACKNOWLEDGMENTS	iv
LIST OF TABLES	x
LIST OF FIGURES	xii
CHAPTER	
I. INTRODUCTION	1
II. BACKGROUND	4
2.1 NEUTRON SOURCE	4
2.1.1 The Ohio State University Research Reactor	4
2.1.2 Thermal Neutron Distribution	7
2.2 TRITIUM PRODUCTION AND DECAY	9
2.2.1 The ${}^6\text{Li}(n,\alpha)$ Reaction	9
2.2.2 Tritium Decay	10
2.3 LIQUID SCINTILLATION COUNTING	12
III. THE DOSIMETRY SYSTEM	15
3.1 THE LITHIUM SOLUTION	15
3.1.1 Choice of a Lithium Compound	15
3.1.1.a Solubility of Lithium Compounds	16

3.1.1.b	Activation of Non-Lithium Elements	17
3.1.2	Unwanted Activations in the Dosimetry Solution	19
3.1.2.a	Hydrogen Activation	19
3.1.2.b	Impurity Activation	20
3.1.2.c	Liquid Scintillation Cocktail Activation	21
3.2	FLUENCE CONSIDERATIONS	22
3.2.1	Gold Wires	22
3.2.2	Uniform Fluence	23
3.2.2.a	Activation of Winding Mechanism	26
3.2.2.b	Time Restrictions	25
3.3	GENERAL PROCEDURES	26
3.3.1	Solution Creation	26
3.3.2	Neutron Irradiation	27
3.3.3	Analysis	28

IV. DEVELOPMENT OF DOSIMETRY SYSTEM

	SPECIFICATIONS	29
4.1	INITIAL EXPERIMENTS	29
4.1.1	Preliminary Activation Trial	29
4.1.1.a	Procedure	30
4.1.1.b	Calculations	30
4.1.1.c	Results	31
4.1.2	Maximum Response Determination	33
4.1.2.a	Procedure	34
4.1.2.b	Calculations	34
4.1.2.c	Results	34
4.2	MAXIMIZING DETECTOR EFFICIENCY	37
4.2.1	Liquid Scintillation Cocktail	37

4.2.2 Scintillation Detector Channel Selection	40
4.2.2.a Pulse Height Analysis	40
4.2.2.b Background Spectrum	42
4.3 IRRADIATION FACTORS	42
4.3.1 Self-Shielding	42
4.3.2 Non-1/v Factor	47
V. SYSTEM EVALUATION	48
5.1 PROCEDURE	48
5.2 CALCULATIONS	49
5.3 RESULTS	52
5.3.1 500 kW	52
5.3.2 50 kW	53
5.3.3 5 kW	54
5.3.4 500 W	55
5.4 ANALYSIS	56
5.4.1 Time Analysis	56
5.4.2 Solution Consistency Analysis	58
5.4.3 Thermal Fluence Analysis	59
5.5 FLUENCE/SAMPLE CPM ₀ RELATIONSHIP	60
5.5.1 Sensitivity	62
5.5.2 Threshold Fluence	62
VI. CONCLUSIONS AND SUGGESTIONS	
FOR FUTURE WORK	63
5.1 CONCLUSIONS	63

BIBLIOGRAPHY	66
APPENDIX A	
MCNP Codes	67
APPENDIX B	
Sample Data	72

LIST OF TABLES

3.1	Solubility Information of Select Lithium Compounds	17
3.2	Cross Sections of Certain Elements	18
3.3	Impurity Activation Information	20
3.4	Contents of Liquid Scintillation Cocktail	21
4.1	Gold Wire Analysis for Preliminary Activation Trial	32
4.2	Preliminary Activation Trial Results	33
4.3	Maximum Response Trial Results	35
4.4	Comparison of Liquid Scintillation Cocktails	39
4.5	MCNP Results	46
5.1	500 kW Results	53
5.2	50 kW Results	54
5.3	5 kW Results	55
5.4	Comparison of Thermal Neutron Fluences	59
B.1	500 kW Sample Data	73
B.2	50 kW Sample Data	74
B.3	5 kW Sample Data	75

B.4 Time And Consistency Analysis Sample Data76

LIST OF FIGURES

2.1	The Ohio State University Research Reactor	5
2.2	Thermal Column Schematic	6
2.3	Typical Maxwellian Distribution	8
2.4	${}^6\text{Li}$ Activation Cross Section	11
2.5	Typical Liquid Scintillation Counter	13
3.1	Gold Activation Cross Section	24
4.1	Relationship Between Lithium Acetate Mass & Detector Efficiency.....	36
4.2	Relationship Between Lithium Acetate Mass & System Response.....	38
4.3	Irradiated Sample Spectrum	41
4.4	Background Spectrum	43
4.5	MCNP Model of Vial	45
5.1	Relationship Between Initial CPM & Thermal Neutron Fluence	61

CHAPTER I

INTRODUCTION

The goal of this research project was to develop a dosimetry system capable of determining a thermal neutron fluence using the ${}^6\text{Li}(n, \alpha)$ reaction and a liquid scintillation counter. The development of the system was divided into three main steps: choosing the system, developing the system specifications, and evaluating the system. The choice of the system depended on two main points:

- (1) The dosimetry system should be able to accurately measure a given incident thermal neutron fluence above some threshold value.
- (2) The system should have good reproducibility. It should be possible to compare data from irradiations that took place at various fluences.

The first criteria assures that a sufficient amount of tritium is produced in each sample for a given irradiation. Two quantities directly control the amount of tritium produced in a given irradiation: the number of ${}^6\text{Li}$ atoms present in the sample, and the magnitude of the incident thermal neutron fluence. Regardless of the mass of lithium compound present in each sample, a threshold fluence will exist below which sample analysis is not possible. As this limit is very important to the feasibility of this dosimetry system, the threshold fluence will be determined. One factor that also may affect the analysis of the dosimetry samples is the production of unwanted radionuclides. For criteria one to be met, the production of all radionuclides other than tritium must be kept to a minimum, while tritium production and detection is maximized.

The second criteria must be met so that the dosimetry system can be used in various different circumstances. Though the data collected from a specific part of the experiment may prove the system works for those particular circumstances, the system must also be reproducible over a wide range of thermal neutron fluences. For the dosimetry system to be practical, the second criteria must be met.

The motivation for this research project was to develop a new kind of thermal neutron dosimetry system. Lithium was chosen for use in this project due to the high thermal neutron activation cross section of ${}^6\text{Li}$. Liquid scintillation counting was chosen for this research to investigate the feasibility of using such a detector for a neutron dosimetry application.

This document covers the development of a thermal neutron dosimetry system. Chapter two of the thesis contains background information related to the project. The source of the thermal neutrons used in the research, details about the reaction between ${}^6\text{Li}$ and thermal neutrons, and a brief introduction of liquid scintillation counters are discussed in this chapter. Chapter three describes the dosimetry system itself. It includes the selection of the lithium compound, details of the irradiations, and the general procedure followed in each part of the experiment. Chapter four contains the preliminary experiments conducted and the steps taken to optimize the dosimetry system. The dosimetry system is evaluated in Chapter five. This chapter describes the experiments conducted to test the system, as well as the results of those experiments. The conclusions of this project and suggestions for possible future study are presented in Chapter six. The appendices contain computer codes and sample data.

CHAPTER II

BACKGROUND

2.1 NEUTRON SOURCE

2.1.1 The Ohio State University Research Reactor

The neutrons used for irradiations in this experiment were provided by the Ohio State University Research Reactor. The Ohio State University Research Reactor (OSURR) is a pool-type 500 kW light water reactor fueled by flat-plate, low enriched (19.5%) uranium silicide rods housed in an aluminum plenum. A simplified layout of the reactor can be seen in Figure 2.1. Graphite reflectors are positioned to the to the south and west of the core [Herminghuysen, 1993]. A graphite thermal column lies to the west of the pool, and an irradiation facility has been created in the column to provide a location suitable for sample irradiation.

Created by removing a number of graphite stringers in the thermal column, the irradiation facility is well suited for irradiation experiments. The open volume created can be seen in Figure 2.2. The 12 inch square by 16 inch deep void was partially filled with a lead shield, creating a 6 inch square opening at the edge of the

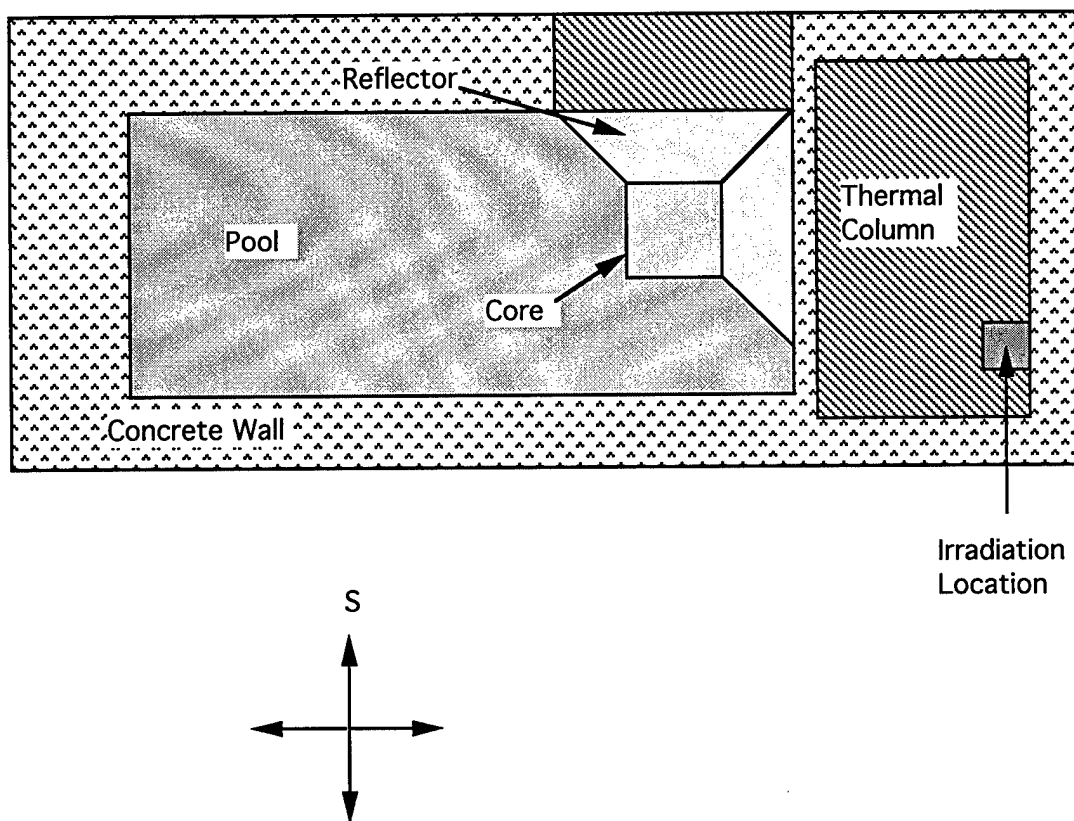


Figure 2.1: The Ohio State University Research Reactor.

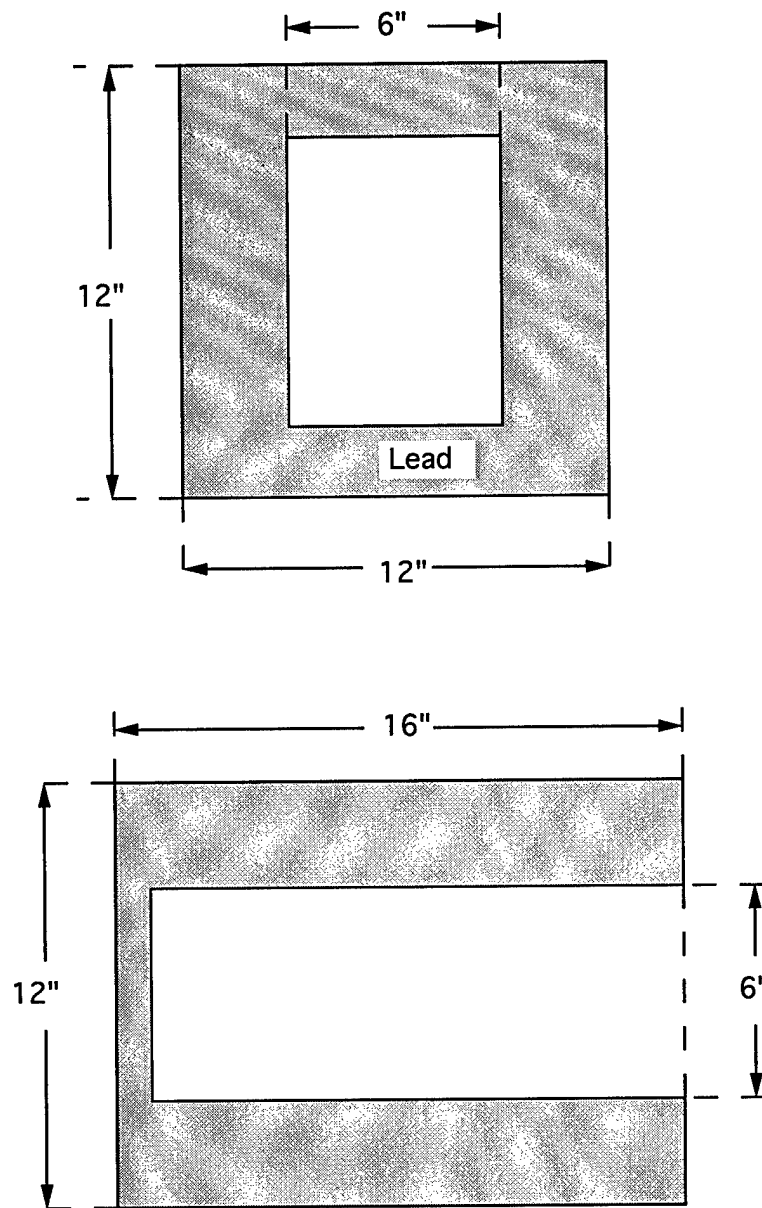


Figure 2.2: Thermal Column Schematic.

thermal column. With the reactor at power, the cadmium ratio (the number of thermal neutrons to epithermal and fast neutrons) in this void was determined to be approximately 390 to 1 [Herminghuysen, 1993].

2.1.2 Thermal Neutron Distribution

The neutron flux in the thermal column was assumed to follow a Maxwellian distribution. If $n(E)dE$ represents the number of neutrons per unit volume with energy in dE about E , then $n(E)$ is given by:

$$n(E) = \frac{n2\pi}{(kT\pi)^{3/2}} E^{1/2} e^{-\frac{E}{kT}} \quad \text{Eq.2-1}$$

where k is Boltzmann's constant, and T is the absolute (Kelvin) temperature of the medium in which the neutrons diffuse [Lamarsh, 1983]. A typical Maxwellian distribution can be seen in Figure 2.3.

It has been proven that for a $1/v$ absorber, the absorption rate is independent of the energy distribution of the neutrons and is determined by the cross section at an arbitrary energy [Duderstadt & Hamilton, 1976]. The arbitrary energy chosen to specify thermal neutron cross sections is $E_0 = 0.0253$ eV, which corresponds to a speed of $v_0=2200$ meters/second. Using a 2200 meter/second cross section to calculate a flux from a reaction rate per unit volume gives a quantity known as the 2200 meter/second flux, ϕ_0 :

$$\phi_0 = nv_0 \quad \text{Eq.2-2}$$

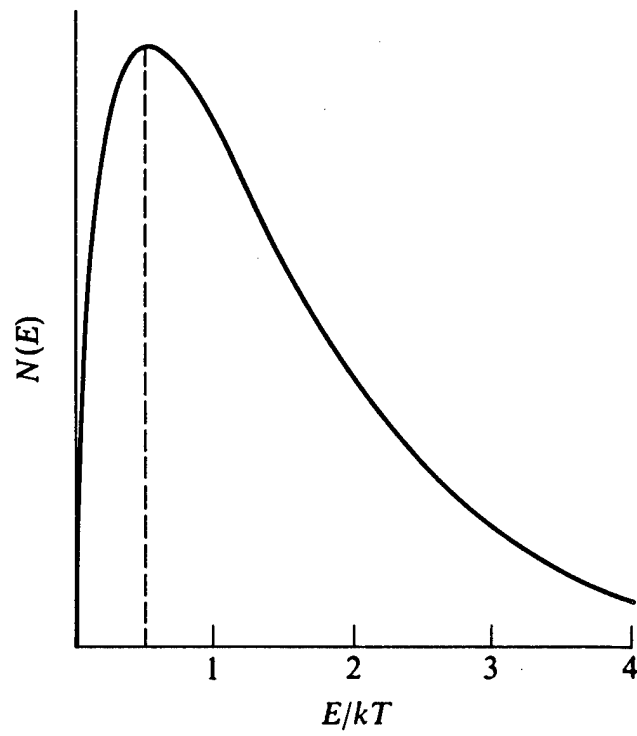


Figure 2.3: A Typical Maxwellian Distribution.

where n is the number of neutrons per cubic centimeter, the integral of $n(E)$ over all energies [Lamarsh, 1983]. Though the temperature in the thermal column was assumed to be 85 °F for each of the irradiations in this research, to keep calculations and discussions simple, the flux discussed in and used in this paper is the 2200 meter per second flux unless specifically noted.

2.2 TRITIUM PRODUCTION AND DECAY

2.2.1 The ${}^6\text{Li}(n, \alpha)$ Reaction

The proposed dosimetry method depends upon the reaction between ${}^6\text{Li}$ and thermal neutrons. This reaction proceeds to the ground state 100% of the time and can be written as:



The thermal neutron cross section (cross section evaluated at $E_0 = 0.0253$ eV) for this reaction is quite large, 945 barns [Hughes & Schwartz, 1958]. The thermal neutron is captured by the nucleus of the ${}^6\text{Li}$ atom, resulting in the production of a tritium atom and the prompt release of an α -particle.

The number of ${}^3\text{H}$ atoms produced in a sample (R) is dependent upon the incident neutron fluence (Φ_0), the absorption cross section (σ), and the number (N) of the ${}^6\text{Li}$ atoms present in the sample to be irradiated. The tritium production reaction

can be symbolized as:

$$R = \Phi_0 N \sigma \quad . \quad \text{Eq.2-4}$$

The relationship between absorption cross section of ${}^6\text{Li}$ and neutron energy can be seen in Figure 2.4. ${}^6\text{Li}$ is a $1/v$ absorber over the energies expected in this research, less than 0.8 MeV [Knoll, 1989]. The large thermal neutron cross section, single absorption product, and $1/v$ absorption characteristics of ${}^6\text{Li}$ were the primary reasons it was chosen for this research project.

2.2.2 Tritium Decay

The tritium, ${}^3\text{H}$, molecule produced in the ${}^6\text{Li}(n, \alpha){}^3\text{H}$ reaction is the product of interest to this dosimetry method. Each thermal neutron absorption produces a single tritium molecule. Tritium decays by emission of a β -particle with a maximum energy of 18.6 keV, and has a 12.4 year half-life. The decay of ${}^3\text{H}$ can be written as:



Due to its long half life, the tritium produced by the absorption of thermal neutrons by ${}^6\text{Li}$ decays at a very slow rate. Sample analysis need not be completed immediately as the tritium produced by an irradiation will stay approximately constant over a reasonable amount of time. The β emissions that do take place, though low in energy, can be recorded by an appropriate detector, such as a liquid scintillation counter. [Knoll, 1989]

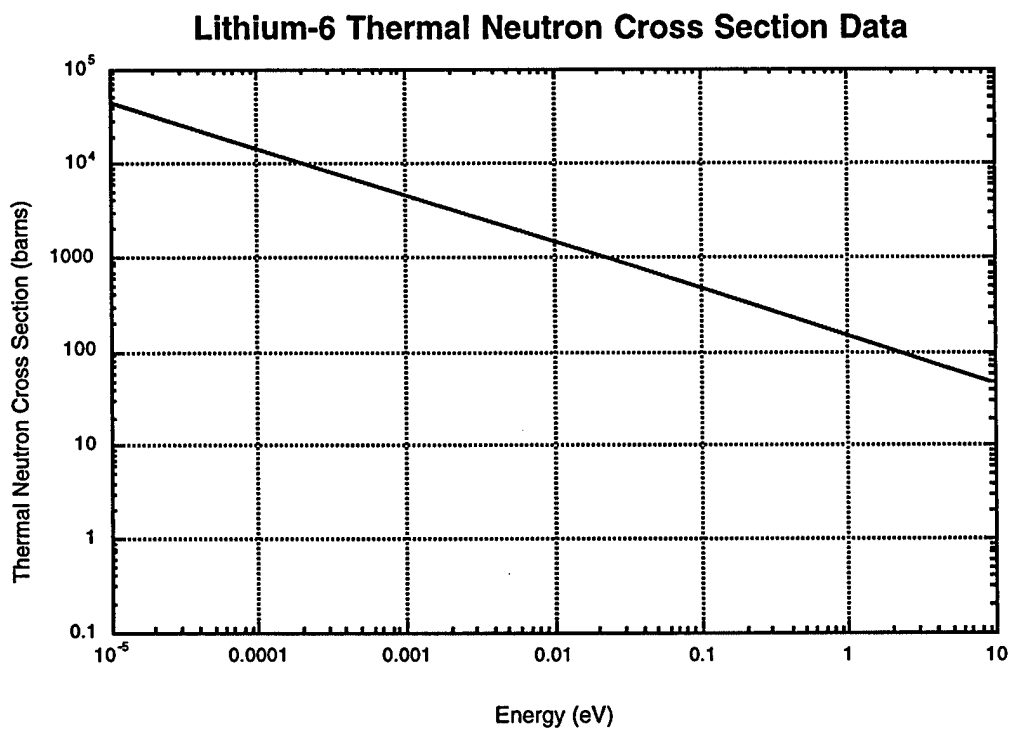


Figure 3.1: ⁶Li Activation Cross Section.

2.3 LIQUID SCINTILLATION COUNTING

One common way to read weak beta emitters such as tritium is to use liquid scintillation counting. In liquid scintillation counting, a radioactive sample is dissolved in a liquid scintillation cocktail containing a mixture of fluors (or scintillators) in an organic solvent [Wang, 1975]. Once properly mixed with the cocktail, the radioactive emissions, specifically β^- emissions, of the radionuclide interact with this mixture in a way that produces small bursts of light.

The process of creating a light pulse from a β^- emission takes many steps. First, the energy of the β -particle is transferred into the surrounding solution, thus exciting the molecules of the solvent. Some of these excited solvent molecules then collide with fluor molecules. Collisions transfer excitation energies to the fluor molecules, and place them in excited states. As an excited fluor molecule loses the excitation energy, each molecule produces one photon of light. [Knoche, 1991] When one of these light photons is incident on the photocathode of a photomultiplier (PM) tube, the counter creates an electrical pulse. If enough light photons simultaneously strike the photocathode of the PM tube, a count may register.

A simplified block diagram of a liquid scintillation counter can be seen in Figure 2.5. The sample to be read is lowered into a chamber and placed close to the photomultiplier tubes. The chamber is dark and shielded, as well as coated with a reflective material to increase the probability of light hitting the PM tubes by

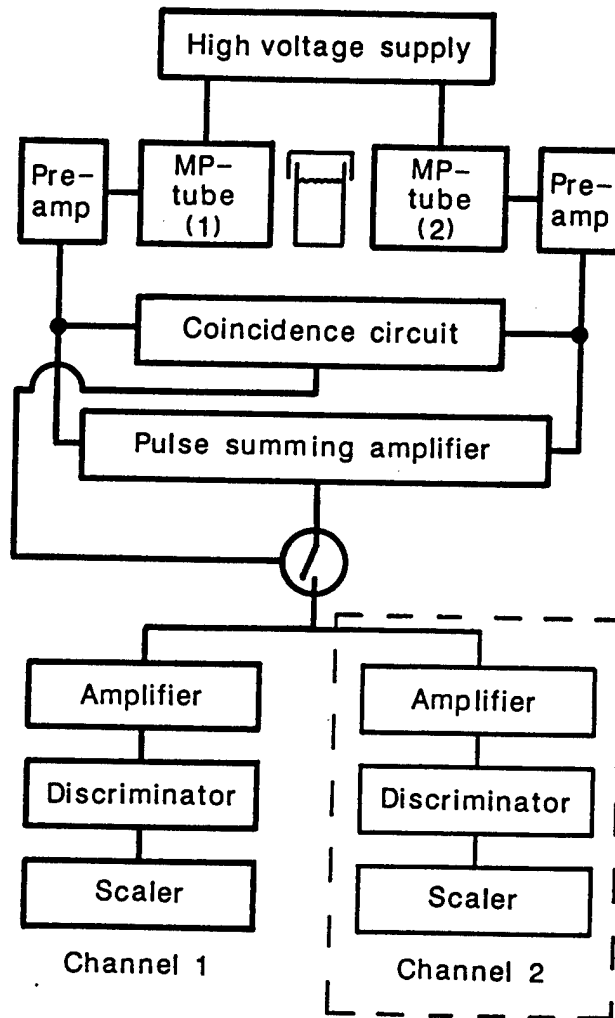


Figure 2.5: A Typical Liquid Scintillation Counter [Knoche, 1991].

reflecting light emissions. PM tubes convert the light emission into an electrical pulse which is then amplified. The amplified pulse is then processed by a multi-channel analyzer (MCA). The MCA allows the discrimination of pulses outside the range set by both a low-level and high-level discriminator. The low-level discriminator removes small pulses of electron noise, while the high-level discriminator removes very large pulses produced by cosmic rays [Knoche, 1991].

One feature that is especially helpful in decreasing background due to PM-tube noise is coincidence counting. As can be seen in Figure 2.5, a coincidence gate blocks the path of electrical pulses produced by the PM-tubes. The gate will complete the circuit, sum the PM-tube outputs, and thus register a count only if both PM-tubes register the radiation simultaneously (or in coincidence). The chance of a both PM-tubes producing a noise pulse at the same time is small, especially if the discriminators are set to remove the weak pulses.

The liquid scintillation detectors used in this study had 1000 channels. Due to its low emission energy, tritium is traditionally counted only in channels 0-400 [Wang, 1975]. In practice, a background count is made with a scintillation solution identical to the samples to be counted, yet without the specific radionuclide present. For this study, the detector channels in the MCA region of interest (ROI) were optimized for the detection of the specific tritium samples. The optimization was based on the measured pulse height spectra for the samples and the background. This optimization is discussed in section 4.3.3.

CHAPTER III

THE DOSIMETRY SYSTEM

3.1 THE LITHIUM SOLUTION

A number of different properties had to be considered to determine the lithium solution best suited for neutron dosimetry by tritium liquid scintillation counting. First, the lithium compound with the most the positive attributes for the dosimetry system had to be found. Next, any negative attributes an aqueous solution of the chosen compound may present, such as the activation of non-lithium solution components, had to be taken into account. These topics are discussed in the following sections.

3.1.1 Choice Of A Lithium Compound

The proposed dosimetry method depends upon finding a lithium compound that holds a number of important qualities. The compound must be highly soluble in water, and the activation of the non-lithium elements in the compound must be minimal. These topics are discussed in the following sections.

3.1.1.a Solubility of Lithium Compounds

In order to prevent the precipitation of solids from the liquid scintillation solution, and to create an aqueous solution rich in ^6Li , a lithium compound with a high water solubility was needed. One milliliter of water was chosen to be used in each sample vial as a compromise between good spatial localization of the fluence and tritium activity for Liquid Scintillation Counting. Thus, a sufficient amount of the compound must be present in each sample to produce an appreciable amount of activity when irradiated.

The compounds considered can be seen in Table 3.1. Though the solubility for lithium carbonate is low, a supply of 93% enriched ^6Li carbonate was available. The enriched lithium carbonate was used as a point of comparison for other compounds. Each of the proposed compounds were analyzed on the basis of the maximum ^6Li mass in 1 ml of water. The natural concentration of ^6Li in lithium in each of the non-enriched compounds was assumed to be 7.5% [Walker, 1989].

Using the information in Table 3.1, one can see that a saturated aqueous solution of lithium chloride will provide the greatest concentration of ^6Li , $2.88\text{E}+21$ atoms per milliliter water. Thus, if solubility were the only property of concern, lithium chloride would be the ideal choice. This is not the case, however, as other factors had to be taken into account including the activation of elements other than lithium.

lithium compound	atomic weight (g)	solubility (g/ml H₂O)	⁶Li atoms per 1 ml H₂O
acetate	102.02	3.00	1.53E+21
bromide	86.85	1.45	8.70E+20
bromide dihydrate	122.88	2.46	1.04E+21
carbonate (93%)	73.89	0.0128	2.24E+20
chlorate	90.39	5.00	2.88E+21
iodide	133.84	1.65	6.43E+20

Table 3.1: Solubility Information of Select Lithium Compounds[CRC, 1985].

3.1.1.b Activation of Non-Lithium Elements

An important property that had to be considered in regards to this dosimetry system was the activation potentials of the non-⁶Li elements in the lithium compound of choice. The proposed dosimetry system depends on the activation of ⁶Li. Ideally, none of the other elements in the chosen lithium compound will react with thermal neutrons. Thus, the thermal neutron cross sections for the non-lithium elements in the chosen compound must be minimal, if not zero. A listing of the elements of concern in the proposed compounds can be found in Table 3.2. Lithium-7 is included in the list due to its presence in all of the potential compounds. In the table, "---" represents no measurable cross section.

As one can see, many of the elements have negligible absorption cross sections. Chlorine, however, has quite a large cross section. Natural chlorine is

lithium compound	elements of concern	thermal neutron absorption cross section (barns)
acetate	carbon	---
	hydrogen	0.332
	oxygen	---
bromide	bromine	6.7
bromide dihydrate	bromine	6.7
carbonate (93%)	carbon	---
	oxygen	---
chlorate	chlorine	33.6
iodide	iodine	7
all	lithium-7	---

Table 3.2: Cross Sections of Certain Elements[Hughes & Schwartz, 1958].

approximately 75.77% ^{35}Cl and 24.23% ^{37}Cl . ^{37}Cl has a negligible cross section compared to ^{35}Cl , and thus, the interaction between chlorine and a thermal neutron can be represented by:



Here, ^{36}Cl is produced. ^{36}Cl is a 709 keV maximum β^- emitter with a $3.01\text{E}+05$ year half life [Walker, 1989]. The presence of this radionuclide could interfere with the analysis of the solutions. Thus, even though lithium chlorate has the highest solubility in water, the compound cannot be used for this dosimetry method.

Instead, lithium acetate, $\text{LiC}_2\text{H}_3\text{O}_2\text{-H}_2\text{O}$ has the best combination of properties: a high solubility in water and a low potential for neutron interaction with elements other than ^6Li . Though the potential for unwanted activations is slim,

the possible activation of elements in an aqueous solution of lithium acetate must be analyzed.

3.1.2 Unwanted Activations in the Dosimetry Solution

One question that must be addressed before lithium acetate can be used for the dosimetry method is, "Do other components of the solution activate?". First, will the great amount of hydrogen in both the lithium acetate dihydroxide and the water create any problems? Also, will any of the impurities in the purchased lithium acetate activate? Finally, will the addition of the liquid scintillation cocktail before the irradiations create problems? These concerns are addressed in the following sections.

3.1.2.a Hydrogen Activation

Due to the great amount of hydrogen in the solutions, the activation of hydrogen had to be taken into account. Each of the solutions in the dosimetry system will contain one milliliter of water, and each single molecule of the lithium acetate contains seven hydrogen atoms. The combination of the hydrogen in both the water and in the lithium acetate creates a situation where neutron absorption by hydrogen is very probable.

Fortunately, thermal neutrons interact with hydrogen to produce a prompt gamma and a deuteron, a stable atom, as shown in the reaction:



[Walker, 1989] Thus, though neutron absorption by hydrogen will occur during irradiations, unwanted radionuclides will not be produced, and thus will present no interference with the dosimetry system.

3.1.2.b Impurity Activation

Though the carbon, hydrogen, and oxygen components of lithium acetate may not produce radionuclides that would effect the dosimetry method, the impurities in the compound may. A list of the impurities found in the lithium acetate purchased and their concentrations can be found in Table 3.3 [Hughes & Schwartz, 1958]. Though the possibility of these impurities being activated exists, the low concentrations of these contaminants compared to the concentration of ${}^6\text{Li}$ makes the possibility of these interactions interfering with the dosimetry system negligible.

impurity	maximum concentration (%)	thermal neutron absorption cross section (barns)
chloride	0.0010	33.6
iron	0.0005	2.53
lead	0.0005	0.17
sulfate	0.0025	0.52

Table 3.3: Impurity Activation Information.

3.1.2.c Liquid Scintillation Cocktail Activation

The final component of the dosimetry solution that must be analyzed for potential activations is the liquid scintillation cocktail. The specific cocktail used for this research was Scintiverse E, a product of Fisher Scientific. The main contents of Scintiverse E can be seen in Table 3.4. Composed of organic compounds, the majority of the cocktail is composed of oxygen, carbon, and hydrogen, and thus will not create any unwanted radionuclides. One of the compounds found in the cocktail, however, contains nitrogen.

Compound	Formula	Amount (%)
Xylene	$(\text{CH}_3)_2\text{C}_6\text{H}_6$	60.7
Ethoxylated Nonyphenol (EO-9)	$\text{C}_2\text{H}_5\text{OCH}_2\text{CO}_2\text{C}_7\text{H}_{15}\text{C}_7\text{H}_5\text{OH}$	39.0
2,5-Diphenyloxazole	$(\text{C}_6\text{H}_5\text{OH})_2\text{C}_3\text{H}_3\text{NO}$	0.5

Table 3.4: Contents of Liquid Scintillation Solution.

The presence of nitrogen in the dosimetry solution during irradiation could interfere with the dosimetry system. Nitrogen has a thermal neutron absorption cross section of 1.7 barns. The reaction between nitrogen and a thermal neutron is:



The product of the reaction, ${}^{14}\text{C}$ is a radionuclide that decays by the emission of a 153-keV β -particle [Walker, 1989]. Even though the β energies of ${}^{14}\text{C}$ decay and

^3H are very different, the presence of ^{14}C could interfere with the dosimetry method. There is no benefit to having the scintillation cocktail in the dosimetry solution at the time of irradiation, and the cocktail can easily be added post irradiation. Thus, it was decided that the scintillation cocktail would be added to the aqueous lithium acetate solution post-irradiation.

3.2 FLUENCE CONSIDERATIONS

Before the irradiations of the samples could begin, two specific topics involving the thermal neutron fluence had to be addressed. First, a way to determine the fluence had to be found. Also, all of the samples in an irradiation had to receive the same fluence. These subjects are addressed in the following sections.

3.2.1 Gold Wires

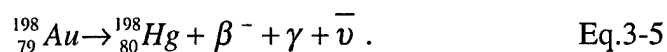
In order to determine the relationship between the thermal neutron fluence and the detected radioactivity, the neutron fluence during the irradiations had to be known. Gold wires were placed in the thermal column along with the samples. These wires were attached to the outsides of the sample vials so that the wires would receive the same fluence as the dosimetry solutions. Thermal neutrons activate gold, and analysis of the resulting radioactivity was used to determine the thermal neutron fluence.

Natural gold, ^{197}Au , activates to form ^{198}Au , a radioactive isotope of gold. The reaction can be represented as:



[Walker, 1989] As discussed in Chapter II, the assumption was made that the flux in the thermal column follows a Maxwellian distribution. The relationship between the absorption cross section of gold and the energy of the incident neutrons can be seen in Figure 3.1. One can see that the relationship approximately follows $1/v$ for the range of energies expected. Thus, the 2200 meter per second cross section, 98.7 barns, was used in the gold wire analysis.

Once each irradiation had taken place, the gold wires were analyzed using a high purity germanium counter. ${}^{198}\text{Au}$ decays by β^- emission:



The wires were counted until the statistical error in the peak counts was less than 1%. The specific activities of the samples were then used to compute the total fluence incident on the samples. Unfortunately, the half-life of ${}^{198}\text{Au}$ is 2.694 days, so the gold samples had to be counted soon after irradiation [Walker, 1989]. Even though the fluence incident on each individual sample could be determined, it was decided that the samples should all be irradiated to the same total fluence.

3.2.2 Uniform Fluence

In order to assure that each sample vial received the same fluence, a device capable of “spinning” the samples as they were irradiated had to be found. A plastic turntable with a copper winding mechanism was chosen to spin the samples. Two problems had to be resolved in spinning the samples. First, activation of the device

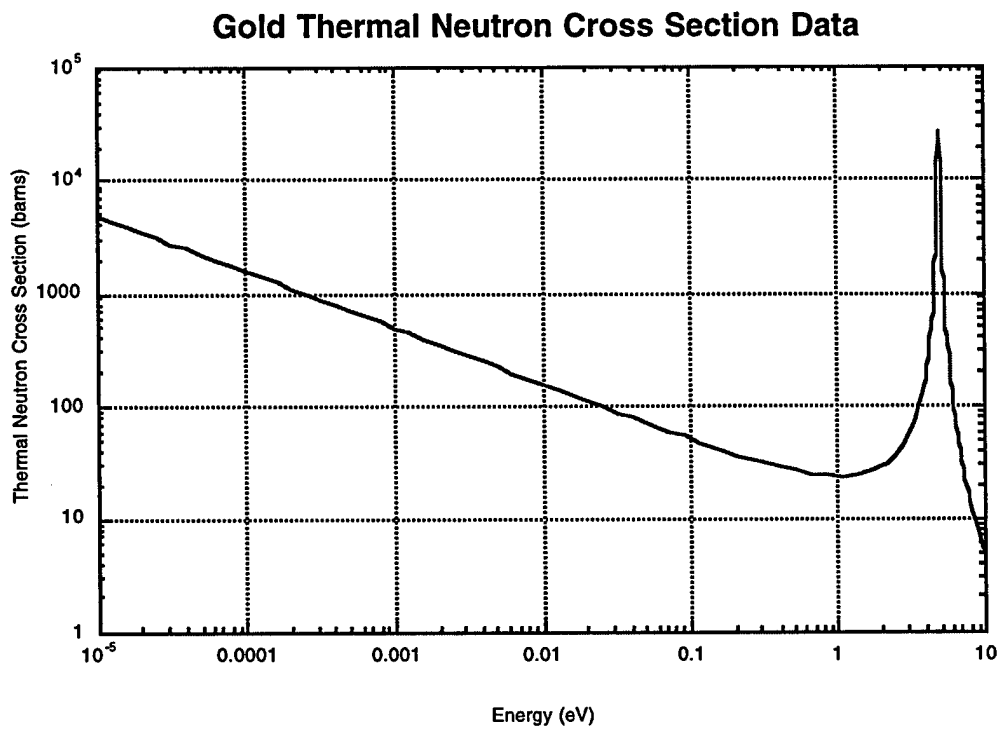


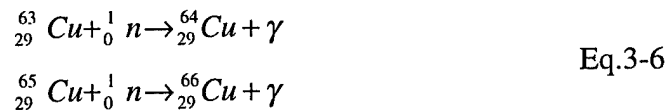
Figure 3.1: Gold Activation Cross Section.

had to be minimal. Also, the samples had to be spun for a long enough time for timing errors in the irradiation period to be small and through enough revolutions for the samples to have all traveled through approximately the same path.

3.2.2a Activation of Winding Mechanism

Since the turntable consists mostly of plastic, it was not anticipated that it would significantly activate in the neutron flux of the thermal column for an irradiation period of less than 30 minutes. This was proven to be the case through experimentation. The assumption was made, however, that the copper winding mechanism would activate. It was unclear whether the activation would be so great as to be an operational problem.

Natural copper consists of two different isotopes, ^{63}Cu (69.17%) and ^{65}Cu (30.83%). The thermal neutron activation cross sections are 4.5 barns and 2.17 barns, respectively. The activation of copper can be represented as:



Fortunately, the half lives of ^{64}Cu and ^{66}Cu are short, 12.7 days and 5.10 minutes respectively [Walker, 1989]. Though the copper would activate, the radioactivity of the winding mechanism would be negligible after few months, so the turntable was suitable by activation standards. Also, the hazard created by the activated copper was minimal. Samples could be recovered from the turntable immediately after irradiation.

3.2.2b Time Restrictions

Due to the fact that the thermal column could not be opened during reactor operation, the turntable had to be able to revolve under its own power for the full irradiation time. It was found that the turntable could revolve for approximately 40 minutes with a single winding. The samples rotated approximately once every 2 minutes 23 seconds, and the irradiation times were set to be approximately 23 minutes, 10 rotations. The concept was that by moving the samples through the same path, each of the irradiated vials received a comparable amount of thermal neutrons, and during the irradiation the fluence incident on each of the vials was assumed to be equal. With 10 revolutions of the turntable, the effect of an incomplete revolution was judged to be acceptable.

3.3 GENERAL PROCEDURES

This section describes the steps taken for each separate irradiation trial in the development of the dosimetry system. Each trial consisted of three main steps: the creation, irradiation, and analysis of the solutions.

3.3.1 Dosimetry Solution Creation

To create the dosimetry solutions, a number of different steps were followed. Each scintillation vial was weighed using a Mettler HL52 scale. The error on each measurement was ± 0.1 milligram. The mass of lithium acetate desired was placed on a filter paper and weighed. Once the lithium acetate was

added to the vial, the mass of the compound was checked by subtracting the mass of the vial from the mass of the filled vial.

After the correct amount of lithium acetate was added to each vial, water was added. One milliliter of demineralized doubly distilled water was added to each vial, regardless of the amount of solid. A Wheaton 100-1095 μl pipetter was used to transfer the water. The error on each pipetting was $\pm 0.6\%$. The vials were then sealed with their caps and were ready to be irradiated.

3.3.2 Neutron Irradiations

As noted in Chapter II, the OSU research reactor was used to irradiate the dosimetry solutions. The reactor was brought up to power at approximately 1 watt. Gold wires were attached to the surfaces of four vials in order to later determine the thermal neutron fluence. The samples were placed on the perimeter of the turntable surface with the turntable fully wound and sitting in the thermal column. As the turntable began to spin, the thermal column was sealed, and the reactor was brought up to the specific power level desired. Each irradiation lasted 23 minutes, approximately 10 revolutions of the turntable.

Once the irradiation was complete, the reactor was turned off, and the samples were retrieved. A survey meter was used to assure that there was no contamination on the vials. The gold wires were removed, and the liquid scintillation cocktail was added to each vial by 10 milliliter pipette with an error of $\pm 2\%$. The vials were then sealed and ready for analysis.

3.3.3 Analysis

Both the dosimetry solutions and the gold wires were analyzed for each trial. The dosimetry solutions were analyzed using a Beckman LS6000TA liquid scintillation counter. Due to chemiluminescence and phosphorescence, the samples were allowed to sit in the liquid scintillation counter bin for a minimum of a 4 hours before they were read. The gold wires were analyzed using a high purity germanium counter as detailed in Section 3.2.1.

CHAPTER IV

DEVELOPMENT OF DOSIMETRY SYSTEM SPECIFICATIONS

Once the dosimetry system was selected, the system had to be optimized by determining any interfering or modifying inputs. In this chapter, the specific experiments which were completed towards this goal, as well as the results of those experiments, are discussed. In order to reduce the relative error in the measured dose, several steps were taken to maximize the detection efficiency of the dosimetry system. Also, two factors involving the irradiation of the dosimetry sample are investigated.

4.1 INITIAL EXPERIMENTS

4.1.1 Preliminary Activation Trial

In order to test a number of the assumptions made in the previous sections, a preliminary activation experiment was completed. The experiment was set up to confirm that the turntable would function as expected, to receive a general idea of the flux in the thermal column, and to assure that the lithium acetate would

indeed activate to produce tritium. The procedure followed and the results of the trial are detailed below.

4.1.1a Procedure

The test consisted of setting eight vials on the turntable, and irradiating the vials for 23 minutes at 50 kW power. It was determined that an aqueous solution of lithium acetate would be heterogeneous if it consisted of greater than 1 milligram lithium acetate. Thus, the four vials with solution contained one gram of lithium acetate dissolved in one milliliter of water, while the other four vials contained only gold wires. The general experimental procedure outlined in section 3.3.1 was followed.

4.1.1b Calculations

To compare the results from the individual samples, an efficiency calculation was completed. The calculations discussed in Section 2.2.1 were followed to calculate the number of tritium atoms produced in each sample, R_0 :

$$R_0 = \Phi_0 N \sigma . \quad \text{Eq.4-1}$$

Here Φ_0 is the 2200 meter per second neutron fluence determined by the analysis of the gold wires used in each irradiation, σ is the ${}^6\text{Li}$ thermal neutron absorption cross section, 945 barns, and N is the number of the ${}^6\text{Li}$ atoms in the dosimetry solution, approximately $4.43\text{E}+20$ atoms.

Once the amount of tritium produced in each sample was determined, the sample activity at the time of analysis had to be calculated. The simple radioactive decay equation:

$$A = \lambda R_0 e^{-\lambda t} \quad \text{Eq.4-2}$$

where λ , the decay constant for tritium ($1.06\text{E-}07$ /minute), was used to calculate sample activity at t , the time of analysis.

Once the activity at the time of analysis was known, the efficiency could be calculated. To obtain a true reading of sample activity, a background counts per minute (BG) was subtracted from all of the analysis data before the efficiency calculation. The background was determined to be 7.47 ± 0.13 counts per minute. Percent efficiency (ϵ) was then calculated as:

$$\epsilon = \frac{CPM - BG}{A} * 100 \quad \text{Eq.4-3}$$

where CPM is the counts per minute for the sample and A is the calculated activity of the sample at the time of analysis in decays per minute.

4.1.1c Results

Though the results confirmed all the preliminary assumptions, the results of the preliminary activation experiment were still mixed. The first concern was the performance of the turntable. The turntable continued to turn for the entire irradiation time, and so it could be assumed that the samples received approximately

Wire Position	2200 m/s fluence Φ_0 ($\times 10^{11}$ /cm ²)
Between vials 1 & 2	3.69
Between vials 2 & 3	3.75
Between vials 3 & 4	3.70
Between vials 4 & 1	3.71

Table 4.1: Gold Wire Analysis for Preliminary Activation Trial.

the same fluence. The results of the gold wire analyses also supported this conclusion. The results of the wire analysis can be seen in Table 4.1. The average fluence for the trial was 3.71×10^{11} n/cm², and the fractional standard deviation was 0.7%. Thus, it appeared that the incident fluence was indeed relatively equal for each of the vials, and the assumption that the gold wires could be used to determine the fluence was confirmed.

Though the results for the analysis of the dosimetry solutions continued to prove the assumption that each of the vials received approximately the same thermal neutron fluence, the analysis of the samples themselves created other concerns. The trial did indeed prove that the samples were activated. The sample data for the preliminary activation experiment can be seen in Table 4.2. The average counts per minute (cpm) detected was 200.6 cpm with a standard deviation of 3.7 cpm. Since the CPM detected from three out of the four samples were within one standard deviation of the mean, and the final sample was within two standard deviations, the

sample	net CPM	DPM expected	efficiency(%)
1	194 ± 2	14090	1.37 ± 0.02
2	190.5 ± 0.9	14060	1.36 ± 0.01
3	198.9 ± 0.4	13980	1.42 ± 0.01
4	190.0 ± 0.5	13970	1.36 ± 0.01

Table 4.2: Preliminary Activation Trial Results.

samples were proven to be statistically equal. Thus, it could be assumed that the dosimetry solutions did indeed receive the same fluence and consequently produced approximately the same amount of tritium. The liquid scintillation counter efficiencies for the samples, however, created concern.

As seen in Table 4.2, the efficiencies of the samples were very low, 1.38 % on average. It was apparent that the lithium acetate solution was causing a great deal of interference in the scintillation process described in Chapter II. The assumption was made that the amount of lithium acetate in each vial not only effected the amount of tritium produced, but also the detector efficiency and response. In order to receive the best statistics possible with this dosimetry system, it was decided that the mass of lithium acetate in milliliter of water that gave the greatest response should be determined.

4.1.2 Maximum Response Determination

In order to determine the mass of lithium acetate that gave the greatest response to a given thermal neutron fluence, a maximum response trial was

completed. The goal of this trial was not to find the mass that gave the best efficiency, but the mass that resulted in the greatest detected counts for a given fluence. A decrease in efficiency was acceptable as long as the detector was able to analyze a greater percentage of the emissions for a given sample and fluence due to the production of more tritium.

4.1.2a Procedure

For this trial, different amounts of lithium acetate were placed in vials along with one milliliter of water. The lithium acetate masses ranged from 0.1 g to 1g. Gold wires were attached to the exterior of four of the vials. The experimental procedures outlined in Section 3.3.1 were followed. The samples were irradiated for 23 minutes at 500 kW.

4.1.2b Calculations

The same equations used in the preliminary activation experiment were used in the maximum response experiment.

4.1.2c Results

The analysis of the Maximum Response Trial solutions proved that the amount of lithium acetate in the dosimetry solution greatly affected the response and efficiency of the dosimetry system. Gold wires again proved that each of the samples received approximately the same fluence. The average 2200 meter per second fluence incident on each vial was determined to be $3.70\text{E}+12 \pm 3\text{E}+10$,

approximately one order of magnitude greater than the fluence used in the previous trial.

As can be seen in Table 4.3, varying the amount of lithium acetate in the dosimetry solution created two distinct noticeable trends. First, the efficiency of the samples decreased as the mass of lithium acetate in the sample increased. The presence of lithium acetate works as a quenching agent during sample analysis, and interferes with the process of light emission as detailed in section 2.3. Increasing the amount of quenching agent correspondingly decreased the efficiency of the sample. The relationship between lithium acetate mass and sample efficiency can be seen in Figure 4.1.

sample	lithium acetate mass (g)	net CPM detected	DPM	detector efficiency (%)
MR-1	0.1	4170	1.73E+4	24.0
MR-2	0.2	4420	3.26E+4	13.5
MR-3	0.3	3170	5.00E+4	6.3
MR-4	0.4	1580	6.52E+4	2.4
MR-5	0.5	1520	8.32E+4	1.8
MR-6	0.6	1600	9.89E+4	1.6
MR-7	0.7	1660	1.16E+5	1.4
MR-8	0.8	1800	1.32E+5	1.3
MR-9	0.9	1830	1.49E+5	1.2
MR-10	1.0	1850	1.65E+5	1.1

Table 4.3: Maximum Response Trial Results.

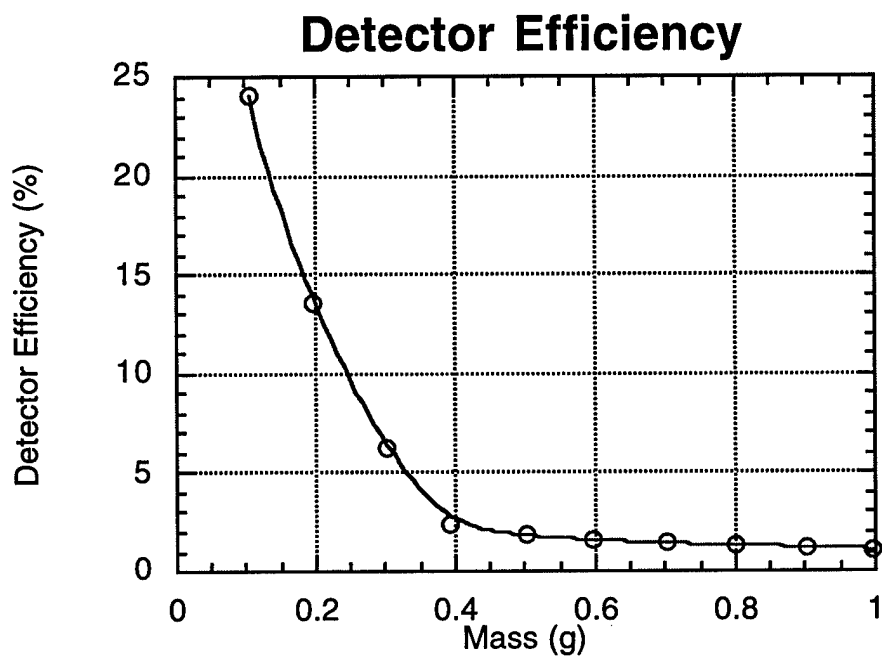


Figure 4.1: Relationship Between Lithium Acetate Mass & System Efficiency.

The other pertinent trend noticeable in Table 4.3 is that as the mass of lithium acetate increases, the response has a noticeable maximum, and then tends to decrease. Since this dosimetry system depends on the events detected by a liquid scintillation counter, the optimum mass of lithium acetate is the amount that gives the greatest response to a given thermal neutron fluence. The relationship between lithium acetate mass and detector response can be seen in Figure 4.2. The mass that generated the greatest response in this trial was approximately 0.2 grams of lithium acetate per milliliter water, corresponding to $8.86\text{E}+19$ atoms of ${}^6\text{Li}$ per milliliter water. This was the concentration of lithium acetate used in the dosimetry system.

4.2 MAXIMIZING DETECTOR EFFICIENCY

As the preliminary trials proved, the efficiency of the dosimetry system was poor. A number of different steps were taken to improve the efficiency of the dosimetry system. These steps are outlined below.

4.2.1 Liquid Scintillation Cocktail

Due to the low efficiencies of the preliminary experiment trials, it was decided to test the liquid scintillation cocktail and determine if the cocktail was performing properly. To achieve this goal, a number of different steps were taken. A different liquid scintillation cocktail was tested, and samples spiked with tritium were created using both the new and test cocktails.

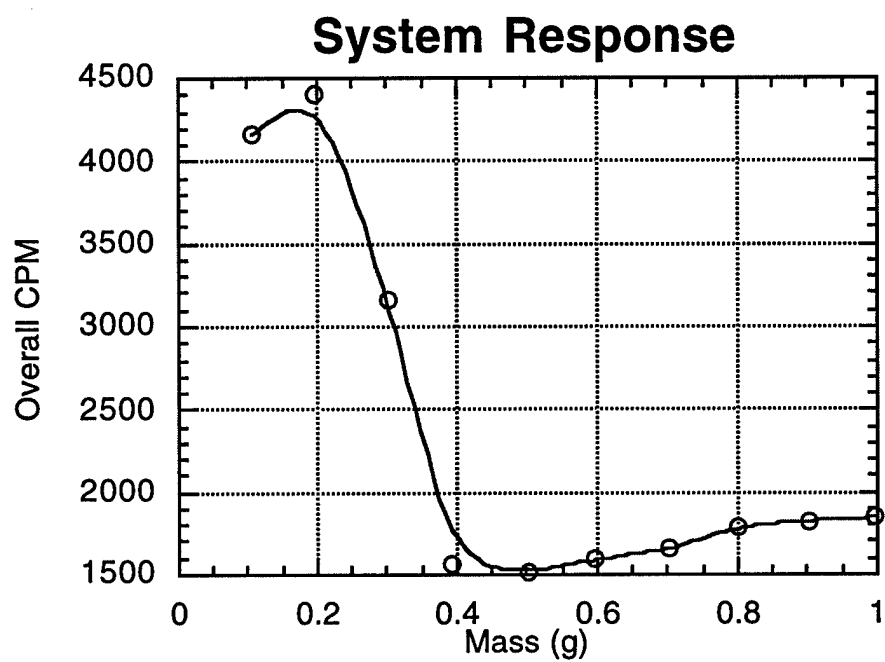


Figure 4.1: Relationship Between Initial CPM & Thermal Fluence.

sample activity	cocktail used	efficiency (%)
76.8 nCi	Scintiverse E	16.8 ± 0.6
76.8 nCi	3a70B	24.8 ± 0.2

Table 4.4: Comparison of Liquid Scintillation Cocktails.

The new liquid scintillation cocktail used was 3a70B, a product of Research Products International Corp. This cocktail is specifically made to give high efficiency with aqueous solutions, and is recommended for use with suspensions. The decision to add the liquid scintillation cocktail to the vials post irradiation remained the same.

To check the efficiency of the liquid scintillation cocktails, spiked samples were created. The samples consisted of 0.2 grams of lithium acetate, 1 milliliter of water, and 3.5 milliliters of cocktail. 0.2 grams of lithium acetate was used because that amount of compound gave the greatest response in the maximum response experiment discussed in the previous section. The water was a combination of the doubly distilled demineralized water used in the previous trials of the experiment and a known amount of tritiated water. Approximately 76 nCi of tritiated water were added to each vial. All of the samples were counted in the traditional tritium window, channels 0-400. Equation 4-3 was used to determine the efficiencies, which can be seen in Table 4.4. Several samples were created using both the

Scintiverse E and the 3a70B scintillation cocktails. The values shown in the table are averages.

One can see that the efficiency of the Scintiverse E cocktail is significantly less than those for the 3a70B cocktail. Due to its higher efficiency with these samples, it was decided to use 3a70B for the remainder of the research.

4.2.2 Scintillation Detector Channel Selection

One final way to improve efficiency was to assure that the correct channels were used during the dosimetry solution analysis with the liquid scintillation counter. To determine the optimum channel selection, two separate counts were taken. A pulse height spectrum of an irradiated sample, and a long background spectrum were taken. The details of these spectra are discussed below.

4.2.2.a Pulse Height Analysis

To find the optimum selection of channels to read the dosimetry solutions, a pulse height analysis of an irradiated sample was completed. The sample contents matched those of the final dosimetry solution: 0.2 grams lithium acetate, 1 milliliter of water, and 3.5 milliliters of 3a70B liquid scintillation cocktail. The resulting spectrum can be seen in Figure 4.3.

One can see that the emission spectrum approximately follows the expected Gaussian form. The traditional tritium counting window is 0-400 channels, and had quenching shifted the tritium emission a significant number of channels, then narrowing our region of interest could have increased the efficiency. Since the

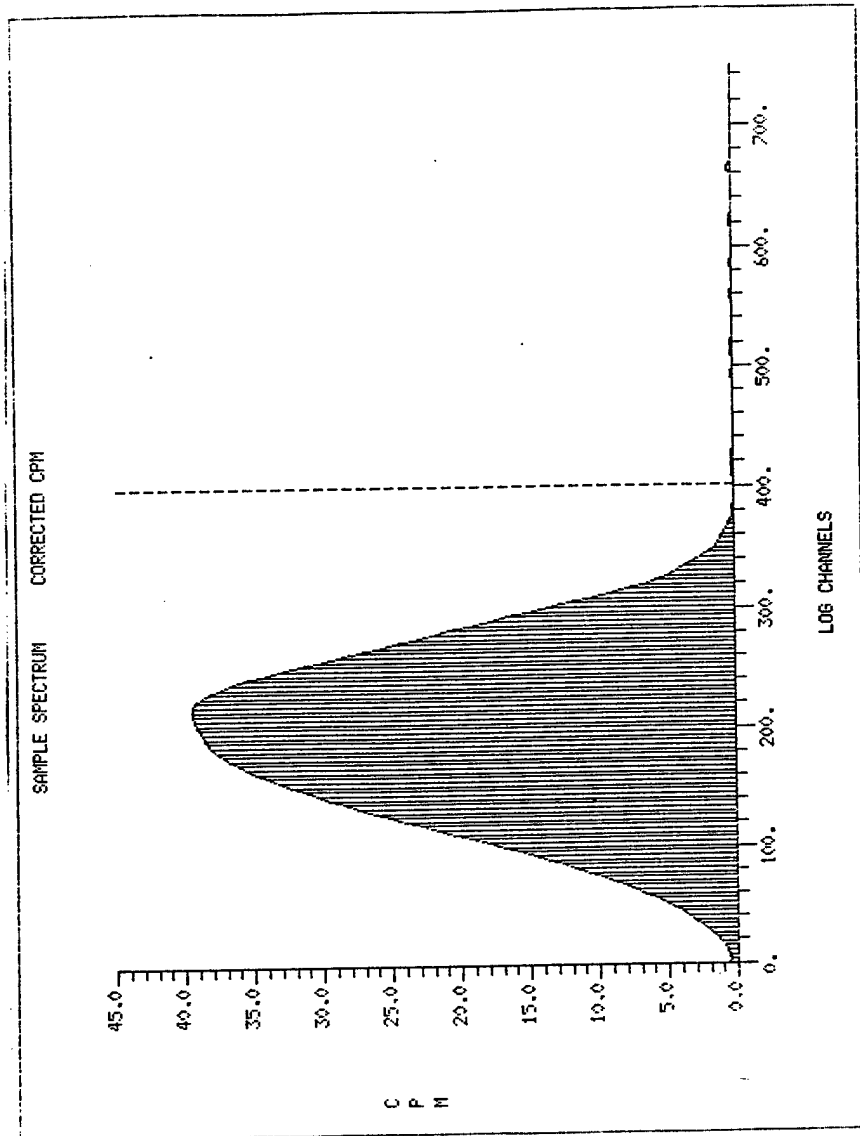


Figure 4.3: Irradiated Sample Spectrum.

emissions fill the first 400 channels, there seems to be no reason to adjust this window. The background spectrum, however, may indeed influence the choice of counting window.

4.2.2.b Background Spectrum

A long (20 hour) background count was taken to determine if background counts were concentrated in any specific channels. The background counts per minute in the tritium window was 12.84 ± 0.02 cpm. An example of a background spectrum can be seen in Figure 4.4. From the figure, one can see, the background counts are distributed over many channels and not concentrated in the first few channels. Also, the liquid scintillation counter which was used had an automatic luminescence compensator to remove the effects caused by spontaneous emissions of light that are detected in spite of the coincidence gate. Thus, it was decided to keep the region of interest for the analysis of samples at 0-400 channels.

4.3 IRRADIATION FACTORS

Two factors important to this dosimetry system that have not been mentioned are the self-shielding factor and the non-1/v factor. Both of these factors affect the system, and must be discussed.

4.3.1 Self-Shielding

One factor that has yet to be addressed is the possibility that the aqueous lithium solution could cause self-shielding. ${}^6\text{Li}$ could absorb neutrons and thereby

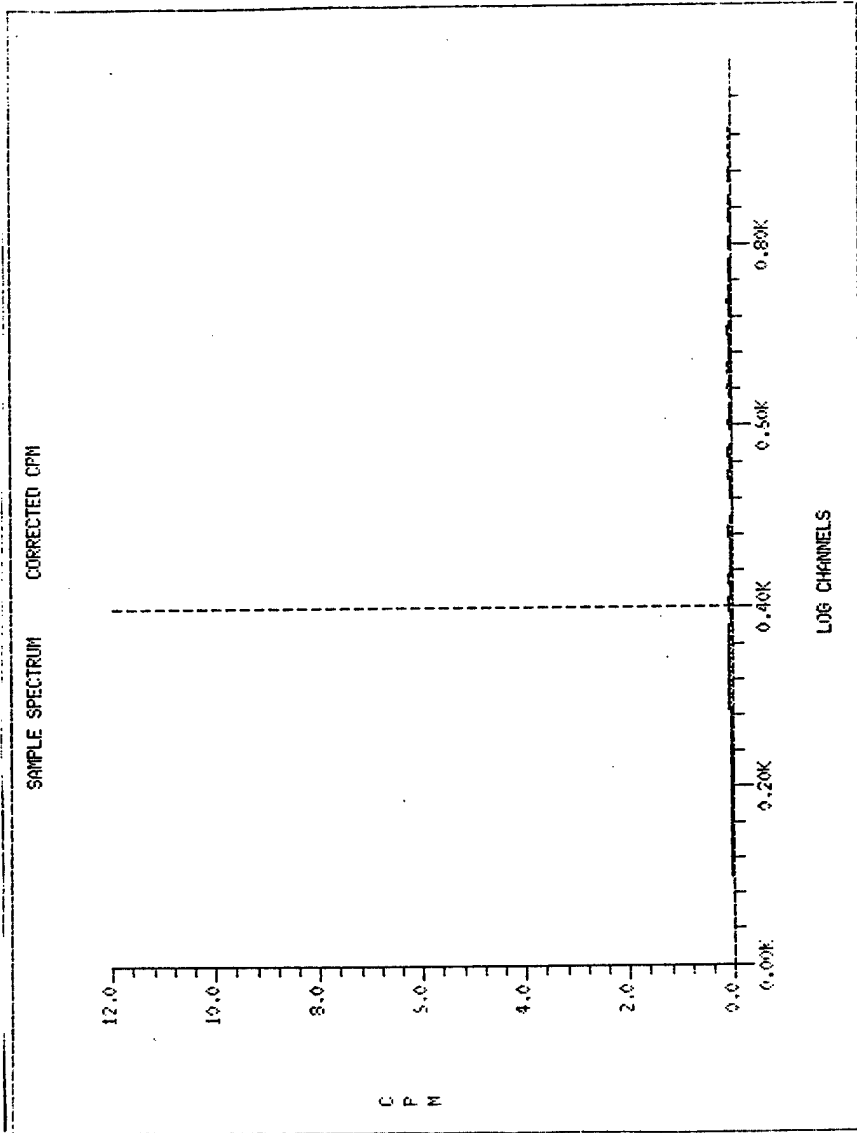


Figure 4.4: Background Spectrum.

decrease the fluence in the vial in comparison to the fluence in air. Also, though the ${}^6\text{Li}$ concentration in the solutions was very small compared to the concentrations of other elements such as hydrogen and oxygen, the presence of these elements could interfere with the activation of the ${}^6\text{Li}$ as well by reflecting neutrons back into the air surrounding the vials. In order to calculate the magnitude of this interference, an MCNP program was created.

MCNP (Monte Carlo N-Particle) is a computer code for analyzing interactions of different types of radiation with computer modeled objects. To determine the amount of self shielding occurring in the sample vials, two similar yet separate models were created. In one, a scintillation vial was modeled with the dosimetry solution present to determine the flux within the solution volume. A picture of this model can be seen in Figure 4.5. The other model consisted of the same vial with the dosimetry solution absent. The same cylindrical volume was monitored in the vial, so that a comparison could be made between the flux in the empty vial and the flux in the dosimetry solution. Copies of the MCNP codes used can be found in Appendix A.

The thermal neutron flux in the thermal column was approximated as a spherical neutron source surrounding each individual vial. The code neutrons were programmed to have the same Maxwellian energy distribution as the neutrons in the thermal column.

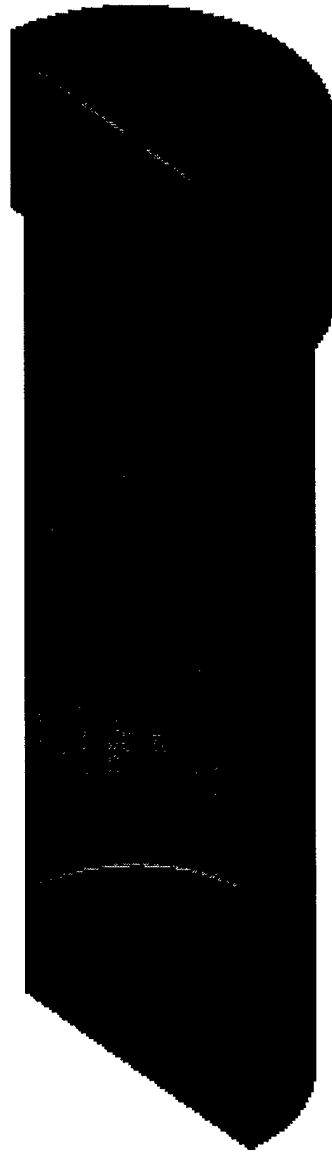


Figure 4.5: MCNP Vial Model

flux in empty vial (n/cm ² s)	flux in vial w/solution (n/cm ² s)	ratio
3.14E-03	2.92E-03	1 to 0.93

Table 4.5: MCNP Results.

Comparison of the MCNP results for the empty and filled vials showed that self shielding was indeed affecting the activation of the ⁶Li in the solution. The fluxes detected in the respective vials can be seen in Table 4.5. Thus, the number of tritium atoms produced in any given irradiation is influenced by self shielding.

As self shielding was present in the irradiation of the dosimetry solutions, a self shielding factor, f_s , must be applied to Equation 2-4, where f_s is defined as:

$$f_s = \frac{\phi_{\text{solution}}}{\phi_{\text{empty}}} . \quad \text{Eq.4-4}$$

The number of tritium atoms produced in a sample (R_0) as found by Equation 2-4 is altered by f_s to give the relation:

$$R_0 = f_s \Phi_0 N \sigma . \quad \text{Eq.4-5}$$

Thus, as self-shielding affects the thermal neutron fluence in the sample vials, the self-shielding factor must be used to account for the difference between the fluence in the air and the fluence in the solution. This factor, however, may not be the only important irradiation factor.

4.3.2 Non-1/v Factor

Another factor that has yet to be taken into account is the fact that gold is not a true 1/v absorber. The relationship between the thermal neutron cross section of gold and the energy of the neutron can be seen in Figure 3.1. The non-1/v factor (g_a) for gold is 1.005 [Profio, 1976]. The 2200 meter per second fluences reported in the previous sections did not take this factor into account. Thus, if Φ_R was the fluence reported by the gold wire analysis, the true 2200 meter per second fluence, Φ_0 , can be found using:

$$\Phi_0 = \frac{\Phi_R}{g_a} = \frac{\Phi_R}{1.005} \quad \text{Eq.4-6}$$

By correcting for the non-1/v factor, the true 2200 meter per second fluence can be reported and used in calculations.

CHAPTER V

SYSTEM EVALUATION

In the last few chapters, a thermal neutron dosimetry system was introduced and modified. In this chapter, this system will be evaluated. First, the details of the experiments conducted will be described. Next, the results of these experiments will be discussed from a number of different perspectives.

5.1 PROCEDURE

To evaluate the system, a number of different irradiations were performed at different fluence levels. Each of the irradiations followed the general procedure described in Section 3.3.1, and was conducted with the OSURR at a different power level. Two trials were completed with the reactor at maximum power, 500 kW. The power for each set of irradiations following was an order of magnitude less. Thus, trials were conducted at 50 kW, 5 kW, and 500 W. All irradiations lasted 23 minutes at the desired power level.

A total of nineteen samples were irradiated for the trials in the kilowatt power range, and only ten samples were irradiated at 500 W. Each sample vial

contained approximately 0.2 grams of lithium acetate, and 1 milliliter of demineralized doubly distilled water. A gold wire was attached to the outside of four vials in the first set of irradiations, and three outside gold wires and one gold wire placed inside of an empty vial were used in the second set of trials. 3.5 milliliters of 3a70B liquid scintillation cocktail were added to each of the vials post-irradiation.

5.2 CALCULATIONS

As discussed in section 3.3, the overall purpose of this dosimetry system is to determine the thermal neutron fluence. To achieve this goal, the detector response function, the relationship between the detected activity of tritium atoms produced in an irradiation and the thermal neutron fluence, was determined. A number of steps were taken to calculate the thermal fluence associated with a specific irradiation.

The activity of a given irradiated sample at the time of analysis (A) can be found using the CPM detected for that sample and the average efficiency of the spiked samples (ϵ_s). As discussed in chapter 4, ϵ_s was determined to be 24.8 ± 0.2 . Thus A can be found using the equation:

$$A = \frac{(CPM - BG)}{\epsilon_s} * 100 \quad \text{Eq.5-1}$$

where CPM is the counts per minute detected by the liquid scintillation counter for a given sample, and BG is the background counts per minute.

Once the activity at the time of analysis is known, the number of tritium atoms formed during the irradiation (R_0) can be found by solving Equation 4-1 for R_0 :

$$R_0 = \frac{A e^{+\lambda t}}{\lambda} = \frac{A_0}{\lambda} \quad \text{Eq.5-2}$$

where λ , the decay constant for tritium (1.06E-07 /minute), was used to calculate sample activity at t , the time of analysis.

As discussed in section 2.2.1, the number of tritium atoms formed in an irradiation is merely the product of the 2200 m/s fluence (Φ_0), the number of ${}^6\text{Li}$ atoms present in the sample (N), and the thermal neutron cross section (σ). Solving this relationship for Φ_0 :

$$\Phi_0 = \frac{R_0}{N \sigma} \quad \text{Eq.5-3}$$

As discussed in previous sections, to keep things simple the 2200 meter per second fluence (Φ_0) was used for calculations in this research. The 2200 meter per second fluence must be transformed into a thermal fluence (Φ_t). The physical relationship between the 2200 meter per second fluence and the thermal fluence is:

$$\Phi_t = \frac{2}{\sqrt{\pi}} \left(\frac{T}{T_0} \right)^{\frac{1}{2}} \Phi_0 \quad \text{Eq.5-4}$$

where Φ_t is the thermal fluence in the solution, T is the temperature of the irradiation medium in Kelvin, and T_0 is the assumed 2200 meter per second

temperature (20.64 °C) [Duderstadt & Hamilton, 1976]. This relationship can be simplified by using the known temperatures:

$$\Phi_t = \left(\frac{2}{\sqrt{\pi}} \left(\frac{302.55^\circ K}{293.61^\circ K} \right)^{\frac{1}{2}} \right) \Phi_0 . \quad \text{Eq.5-5}$$

The numerical relationship is then:

$$\Phi_t = (1.145)\Phi_0 . \quad \text{Eq.5-6}$$

Both the thermal fluences determined by the gold wires and those calculated using the sample CPM must take other factors into account. The thermal fluences calculated with sample CPM must also take the self-shielding factor into account. As discussed in section 4.3, the irradiated samples in the research project were affected by self-shielding, and thus the calculation of Φ_t in air must take into account the self-shielding factor, f_s .

$$\Phi_t^{empty} = \frac{\Phi_t^{solution}}{f_s} . \quad \text{Eq.5-7}$$

Thus, the thermal fluences in air calculated with the sample CPM's must use the relationship:

$$\Phi(S)_t = \frac{(1.145)\Phi_0}{f_s} = (1.231)\Phi_0 . \quad \text{Eq.5-8}$$

The thermal fluences determined by the gold wires are influenced by the non-1/v factor as discussed in section 4.3. Thus, the thermal fluences in air calculated using the values of Φ_0 reported by the gold wires must use the relation:

$$\Phi(G)_t = \frac{(1.145)\Phi_0}{g_A} = (1.139)\Phi_0 . \quad \text{Eq.5-9}$$

Thus, Equations 5-8 and 5-9 were used to calculate the thermal neutron fluences using data from the sample analysis and gold wire analysis, respectively.

5.3 RESULTS

Each irradiated solution was analyzed by counting the sample twice on two separate occasions for a total of four individual results. The results of these analyses are discussed in the next four sections.

5.3.1 500 kW

Two separate irradiations were conducted with the reactor at full power, 500 kW. Each sample was counted four separate times for a period of 15 minutes. The raw data collected from the liquid scintillation counter for these trials and the preliminary calculations leading to the measured fluences can be seen in Appendix B. The counts per minute for each vial, as determined by the detector, are not directly comparable due to radioactive decay, and thus that information is not presented here. The fluence detected from the analysis of the gold wires, after taking into account the non-1/v factor for gold, and the thermal fluences determined with the individual CPM from each sample can be seen in Table 5.1. The cause of the difference between average sample values will be addressed in section 5.3.

TRIAL ONE		TRIAL TWO	
gold wire thermal fluence $\Phi(G)_t = 3.94E+12 \pm 1E+10 \text{ n/cm}^2$		gold wire thermal fluence $\Phi(G)_t = 3.89E+12 \pm 2E+10 \text{ n/cm}^2$	
sample	sample $\Phi(S)_t * 10^{12}$ (n/ cm ²)	sample	sample $\Phi(S)_t * 10^{12}$ (n/ cm ²)
A-1	3.45 ± 0.03	B-1	3.80 ± 0.03
A-2	3.45 ± 0.03	B-2	3.74 ± 0.03
A-3	3.35 ± 0.03	B-3	3.82 ± 0.03
A-4	3.32 ± 0.03	B-4	3.77 ± 0.03
A-5	3.37 ± 0.03	B-5	3.84 ± 0.03
A-6	3.35 ± 0.03	B-6	3.73 ± 0.03
A-7	3.41 ± 0.03	B-7	3.92 ± 0.03
A-8	3.44 ± 0.06	B-8	3.81 ± 0.03
A-9	3.61 ± 0.04	B-9	3.82 ± 0.03
A-10	3.53 ± 0.03	---	
average	3.43E ± 0.03		3.80E ± 0.02

Table 5.1: 500 kW Data.

5.3.2 50 kW

For the second set of irradiations, the reactor was brought to 50 kW. Each sample was counted four separate times for a period of 30 minutes. The raw data collected from the liquid scintillation counter for these trials and the preliminary calculations leading to the detector efficiencies can be seen in Appendix B. The fluence detected from the analysis of the gold wires, after taking into account the non-1/v factor for gold, and the thermal fluences determined with the individual CPM from each can be seen in Table 5.2.

TRIAL ONE		TRIAL TWO	
gold wire thermal fluence $\Phi(G)_t = 4.36E+11 \pm 1E+09 \text{ n/cm}^2$		gold wire thermal fluence $\Phi(G)_t = 4.09E+11 \pm 1E+09 \text{ n/cm}^2$	
sample	sample $\Phi(S)_t * 10^{11}$ (n/ cm ²)	sample	sample $\Phi(S)_t * 10^{11}$ (n/ cm ²)
A-1	3.03 \pm 0.04	B-1	3.93 \pm 0.04
A-2	3.11 \pm 0.04	B-2	4.00 \pm 0.05
A-3	2.83 \pm 0.03	B-3	3.97 \pm 0.04
A-4	3.00 \pm 0.03	B-4	3.91 \pm 0.03
A-5	2.76 \pm 0.04	B-5	3.92 \pm 0.04
A-6	3.01 \pm 0.03	B-6	3.90 \pm 0.04
A-7	3.08 \pm 0.05	B-7	3.89 \pm 0.04
A-8	2.58 \pm 0.04	B-8	3.99 \pm 0.03
A-9	2.99 \pm 0.04	B-9	4.02 \pm 0.04
A-10	3.25 \pm 0.04	---	
average	2.96 \pm 0.06		3.95 \pm 0.01

Table 5.2: 50 kW Data.

As stated previously, the cause of the difference between the average sample values will be addressed in section 5.3.

5.3.3 5 kW

As with the previous set of irradiations, the reactor power level was again reduced by an order of magnitude for these samples. Thus, the samples were irradiated with the reactor operating at 5 kW. The samples were counted four times for an hour each. Again, the raw data collected from the liquid scintillation counter for this trial and the preliminary calculations leading to the sample thermal fluences can be seen in Appendix B. The pertinent data from this trial can be seen in Table

TRIAL ONE		TRIAL TWO	
gold wire thermal fluence $\Phi(G)_t = 4.01E+10 \pm 2E+08 \text{ n/cm}^2$		gold wire thermal fluence $\Phi(G)_t = 4.12E+10 \pm 1E+08 \text{ n/cm}^2$	
sample	sample $\Phi(S)_t * 10^{10}$ (n/ cm ²)	sample	sample $\Phi(S)_t * 10^{10}$ (n/ cm ²)
A-1	3.59 ± 0.07	B-1	3.90 ± 0.08
A-2	3.58 ± 0.05	B-2	3.93 ± 0.06
A-3	3.65 ± 0.06	B-3	3.81 ± 0.03
A-4	3.27 ± 0.01	B-4	4.03 ± 0.07
A-5	3.25 ± 0.07	B-5	3.90 ± 0.09
A-6	3.28 ± 0.09	B-6	3.90 ± 0.08
A-7	3.38 ± 0.04	B-7	3.88 ± 0.08
A-8	2.75 ± 0.04	B-8	3.75 ± 0.05
A-9	2.99 ± 0.08	B-9	3.88 ± 0.07
A-10	3.48 ± 0.05	---	---
average	3.32 ± 0.09		3.89 ± 0.02

Table 5.3: 5 kW Data.

5.3. The reasons behind the discrepancy between the sample fluence values will be discussed in section 5.3.

5.3.4 500 W

Though the initial irradiations used high power levels and thus high thermal neutron fluences, the samples in the fourth set of irradiations were irradiated with the reactor operating at only 500 W. One important part of this research project was to determine the thermal neutron fluence threshold, the lowest fluence that could be analyzed. Since the power level of the reactor was only 500 W during the

irradiations, the thermal neutron fluence was reported to be only $3.34\text{E}+09 \pm 1\text{E}+07$ n/cm².

Unfortunately, the fluence used for this irradiation is below the threshold of the dosimetry system. Assuming that 0.2 grams were dissolved in each vial, $2.80\text{E}+08$ atoms of tritium would be produced in each vial, corresponding to 29.63 DPM. With the detector efficiency being between 20 - 25%, one can expect to detect a maximum of only 7 cpm from each of these samples. Considering the background reading for the tritium window was 12.84 cpm, the expected activities of these samples would be less than background. Such a small amount of activity over background is not statistically sound, and thus only one set of irradiations were completed at this level. The samples cannot be used in this dosimetry system.

5.4 ANALYSIS

5.4.1 Time Analysis

Comparing the ratio of the thermal fluences from the samples to the thermal fluences from the gold wires ($\Phi(S)_t / \Phi(G)_t$) for each power level, one can see that there appears to be large discrepancies between these ratios for sets A & B for each power level. One piece of information that has to be taken into account is the amount of time that passed between the irradiations of the samples and the analysis of the samples.

Due to limitations of equipment and facilities, the samples from the first set of irradiations (referred to by "A - #") were read an average of 19 days post-irradiation. The second set of samples (referred to by "B - #"), however, were read only a few days post-irradiation. It appears that something is decreasing the detectable emissions of the samples as time passes.

To prove this assumption, the first set of samples ("A" samples) irradiated at 500 kW, originally analyzed 23 days post-irradiation, were read again 37 days post-irradiation. The raw data for this analysis can be seen in Appendix B. As the average thermal fluence of the samples was $3.43\text{E}+12 \pm 0.03 \text{ n/cm}^2$ when read at 23 days, the average thermal neutron fluence dropped to $3.08\text{E}+12 \pm 0.04 \text{ n/cm}^2$ after 37 days, a decrease of over 10%. It appears that as the samples sit over time, the number of detectable emissions from the samples decreases at a rate greater than the simple radioactive decay of tritium.

There are a number of possible explanations for this loss. It is possible that tritium is escaping the scintillation vials both through the seal of the lid and vial, and by migrating through the plastic itself. Also, the liquid scintillation cocktail could be degrading over time.

Regardless of the reasons behind the loss, the samples in the research must not be allowed to sit for a long period of time post-irradiation. To get a true analysis of the samples, they must be read soon after irradiation. Thus, the data obtained in the first set of irradiations (designated with an "A"), must be discarded.

5.4.2 Solution Consistency Analysis

Though time caused the samples to decrease in efficiency, one factor that does not greatly affect the efficiency of the dosimetry samples is the consistency of the solution. Over time, the mixing among the lithium acetate, water, and liquid scintillation cocktail in the dosimetry solutions will gradually change. All the samples analyzed previously were treated identically. The samples were allowed to settle before analysis. Nevertheless, the effects of solution consistency were analyzed as detailed below.

The same samples analyzed for efficiency loss due to time (samples "A", 500 kW), were also used to determine the effects of settling, or more precisely, the effects of not settling. Each of the samples were mixed thoroughly before analysis. The average thermal neutron fluence of the samples after sitting for weeks, as seen in the previous section, was $3.08\text{E}+12 \pm 0.04 \text{ n/cm}^2$. After the samples were well mixed, the average fluence was $3.21\text{E}+12 \pm 0.05 \text{ n/cm}^2$, only a 4% difference. This 4% difference is not sufficient to account for the over 10% difference between the samples analyzed after 15 days. It is clear that the samples are indeed losing detectable emissions. Thus, it was concluded that the dosimetry solution consistency was not the reason behind the great decrease in calculated thermal neutron fluence after days had passed between analysis of samples .

5.4.3 Thermal Fluence Analysis

Equation 5-8 was used to calculate the thermal neutron fluences in air for each set of samples, and Equation 5-9 was used to calculate the thermal neutron fluences using the gold wire data. The results of these calculations, for the second set of irradiations, can be seen in Table 5.4.

trial	$\Phi(G)_i$ gold wire thermal fluence (n/cm ²)	$\Phi(S)_i$ sample thermal fluence (n/cm ²)
500 kW	3.89E+12 ± 2E+10	3.80E+12 ± 2E+10
50 kW	4.09E+11 ± 9E+08	3.95E+11 ± 1E+09
5 kW	4.12E+10 ± 1E+08	3.89E+10 ± 2E+08

Table 5.4: Comparison of Thermal Fluences.

The thermal fluences determined from the samples are consistently less than the thermal fluences determined from the gold wires. The fluences differ by 2%, 3%, and 6% for the three trials. Many different properties of the samples could create this difference. First, the chemical form of the tritium in the spiked samples (tritiated water) is not the same chemical form as the tritium produced in the irradiated samples. Also, the irradiation of the lithium acetate solution could produce a quenching compound of some sort that would interfere with light pulse formation in the samples and thus decrease detector efficiency.

5.5 FLUENCE/SAMPLE CPM₀ RELATIONSHIP

As discussed previously, the final goal of this research project was to determine the relationship between the CPM of an analyzed sample and the thermal fluence associated with the sample. Since the samples in this research must be read promptly to avoid loss of detectable emissions, the CPM of a sample as read can be accepted as the initial CPM of the sample (CPM₀). The long half-life of tritium keeps the activity relatively constant over the span of a few days. The CPM₀ for a given sample was calculated using its initial activity (A₀) found using Equation 5-1. The initial counts per minute is related to A₀ through the relation:

$$CPM_0 = A_0 \frac{\epsilon_s}{100} . \quad \text{Eq.5-10}$$

The average thermal fluences determined by both the samples ($\Phi(S)_i$) and the gold wires ($\Phi(G)_i$) were plotted as a function of the average CPM₀ for each set of irradiations. This relationship can be seen in Figure 5.1. Note that the graph is on a log-log scale.

In each case, the relationship between the CPM₀ and the thermal neutron fluence are linear. The slope of the line is the dosimetry system sensitivity, and will be discussed in the next section. As noted previously, the gold wire thermal fluences are consistently greater than the sample thermal fluences. As one can see in the figure, the difference between the two fluences decreases as the fluence increases.

Thermal Fluence

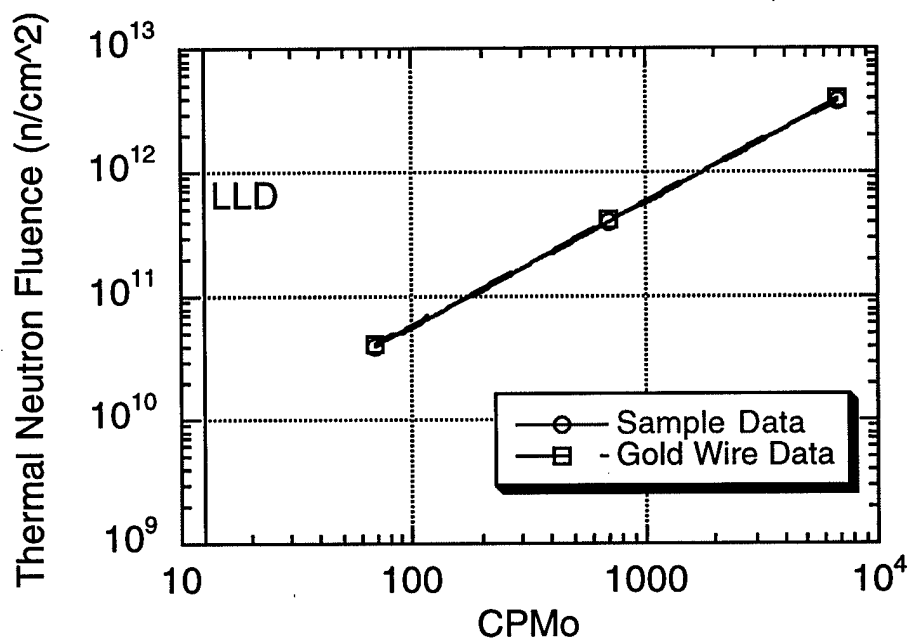


Figure 5.1: Relationship Between Initial CPM & Thermal Fluence.

5.5.2 Sensitivity

The sensitivity of the system is as follows: a $5.64\text{E}+08 \pm 0.04\text{E}+6$ n/cm² increase in thermal neutron fluence is necessary to increase the detectable CPM of the system by 1 cpm. The sensitivity reported is an average of the sensitivities of the gold wire data and sample data.

5.5.2 Threshold

An important property to consider is the threshold thermal neutron fluence of the system, the minimum thermal fluence the system can detect with certainty. As discussed in section 5.2.4, the CPM obtained from the 500 W trial samples were not statistically sufficient. Though the liquid scintillation counter could detect tritium in the samples, the low number of emissions fluctuates greatly between analyses. Two consecutive hour long readings of the same sample resulted in a difference in CPM of over 40%.

To ensure the results of low emission data, the limit of twice background was chosen as the lower limit of detection (LLD) of the system. A sample must have a minimum of 12.84 detectable counts per minute over background to be accepted by this system. This LLD is shown in Figure 5.1. The thermal neutron fluence corresponding to this LLD is approximately $8.1\text{E}+09$ n/cm² using the sample data, and $9.4\text{E}+09$ n/cm² using the gold wire data. Thus, this system should not be used to detect a thermal neutron fluence below $8.6\text{E}+09 + 0.5\text{E}+08$ n/cm².

CHAPTER VI

CONCLUSIONS AND SUGGESTIONS

FOR FUTURE WORK

5.1 CONCLUSIONS

The dosimetry system described in the thesis appears to work. The thermal neutron fluences calculated with the sample CPM's are all within 6% of the fluence determined using the gold wires. The non-linearity of the gold wire results does bring up the possibility that the fluences received from the wire analyses were not correct. Also, the system thermal fluence values were consistently less than the gold wire fluence values.

The LLD of this system was chosen to be twice background, or 12.84 cpm. This LLD corresponds to a thermal neutron threshold of $8.6\text{E}+09 + 0.5\text{E}+08 \text{ n/cm}^2$. An increase of $5.64\text{E}+08 \pm 0.04\text{E}+6 \text{ n/cm}^2$ is necessary to cause the detectable CPM to increase by 1 cpm.

5.2 SUGGESTIONS FOR FUTURE WORK

As it was discovered that the efficiencies of the samples decreased over time, an investigation into the reasons for this loss of detectable emissions could be pursued. A number of possible explanations for this loss were mentioned in section 3.3. Preparing samples with wax sealed vials or vials made from glass are only two possibilities in discovering the reasons for this decrease in efficiency.

The self-shielding factor affected the analysis of the samples in this dosimetry system, yet this factor is good only for the geometry used in this research. To make this project useful over many different situations, the effects of irradiation geometry on the self-shielding factor should be looked into.

One of the procedures not utilized in this research was the use of batch samples. A bulk or batch sample method could be used in two main steps in this research. First, a bulk aqueous lithium acetate solution with the 0.2 gram/milliliter concentration could be created and thoroughly mixed with a magnetic stirring. The individual solutions to be irradiated could be drawn from the bulk solution. Also, solutions of more than 1 milliliter could be irradiated and then individual samples could be pipetted into the scintillation vials.

The use of enriched lithium acetate could increase the sensitivity of this dosimetry system. Increasing the ^6Li concentration in the lithium acetate from 7.5% to over 90% would increase the number of tritium atoms formed in a given

irradiation, and thus increase the number of detectable emissions for a given sample.

BIBLIOGRAPHY

1. Weast, Robert C. ed. "CRC Handbook of Chemistry and Physics". CRC Press, 1985.
2. Duderstadt, James J., and Hamilton, Louis J. "Nuclear Reactor Analysis". John Wiley & Sons, Inc., 1976.
3. Herminghuysen, Kevin. "Development and Evaluation of a Neutron-Gamma Mixed Field Dosimetry System Based on a Single Thermoluminescence Dosimeter". The Ohio State University, 1993.
4. Hughes, Donald, and Schwartz, Robert. "Neutron Cross Sections", Brookhaven National Laboratory, 1958.
5. Knoche, Herman W. "Radioisotopic Methods for Biological and Medical Research". Oxford University Press, New York. 1991.
6. Knoll, Glenn F. "radiation Detection and Measurement". John Wiley & Sons, Inc., 1989.
7. Lamarsh, John R. "Introduction to Nuclear Engineering". Addison-Wesley Publishing Company, Inc., 1983.
8. Profio, A. Edward. "Experimental Reactor Physics". John Wiley & Sons, Inc., 1976.
9. Wang, C.H., Willis, D.L., Loveland, W.D. "Radiotracer Methodology in the Biological, Environmental, and Physical Sciences". Prentice-Hall, Inc., 1975.
10. Walker, F. William. "Nuclides and Isotopes". General Electric Co., 1989.

APPENDIX A

MCNP CODES

Liquid Scintillation Vial - Full

```
c
c *****
c      Cell Cards
c *****
c
5 1 -0.935 10 -20 -30 $ vial bottom
10 1 -0.935 20 -70 40 -30 $ vial side
15 1 -0.935 60 -50 -80 $ lid top
20 1 -0.935 70 -60 40 -80 $ lid side
25 2 -1.2 20 -90 -40 $ solution
30 3 -0.00129 90 -60 -40 $ air
35 3 -0.00129 (-10:50:80:30 -70) -999 $ internal
40 0 999 $ outside
```

```
c
c *****
c      Surface Cards
c *****
c
10 pz 0 $ bottom
20 pz 0.1 $ bottom inner surface
30 cz 0.85 $ outside vial side
40 cz 0.75 $ vial inner surface
50 pz 5.5 $ top
60 pz 5.4 $ top inner surface
70 pz 4.5 $ bottom of lid
80 cz 0.95 $ lid inner surface
90 pz 0.67 $ top of solution
888 so 10 $ source
999 so 50 $ outside world
```

```
c
c *****
c      Problem Type
c *****
```

mode n

```
c
c *****
c      Variance Reduction
c *****
```

imp:n 1 6r 0

```
c
c *****
c      Source
c *****
```

sdef sur=888 nrm=-1 erg=d1

spl -2 2.607E-08

```
c
c *****
c      Tally
c *****
```

```

c
f4:n 25
c
c *****
c      Material
c *****
c
m1 1001.50 0.66667 6012.50 0.33333
m2 8016.50 0.3266 1001.50 0.6432 6000.50 0.0201 3007.55 0.0093 3006.50 0.0008
mt2 lwtr.01
m3 7014.50 0.78457 8016.50 0.21068 18000.35 0.00469 6012.50 0.00006
c
c *****
c      Energy Cards
c *****
c
c
c
c *****
c      Cutoff Cards
c *****
c
prdmp 3j 1
ctme 720
c ptrac file=asc
c
c *****
c      Peripherals
c *****
c
print

```

Liquid Scintillation Vial - Empty

```
c
c *****
c      Cell Cards
c *****
c
5 1 -0.935 10 -20 -30 $ vial bottom
10 1 -0.935 20 -70 40 -30 $ vial side
15 1 -0.935 60 -50 -80 $ lid top
20 1 -0.935 70 -60 40 -80 $ lid side
25 3 -0.00129 20 -90 -40 $detector
30 3 -0.00129 90 -60 -40 $ air
35 3 -0.00129 (-10:50:80:30 -70) -999 $ internal
40 0 999 $ outside
```

```
c
c *****
c      Surface Cards
c *****
c
10 pz 0 $ bottom
20 pz 0.1 $ bottom inner surface
30 cz 0.85 $ outside vial side
40 cz 0.75 $ vial inner surface
50 pz 5.5 $ top
60 pz 5.4 $ top inner surface
70 pz 4.5 $ bottom of lid
80 cz 0.95 $ lid outer surface
90 pz 0.67 $ top of detector
888 so 10 $ source
999 so 50 $ outside world
```

```
c
c *****
c      Problem Type
c *****
```

mode n

```
c
c *****
c      Variance Reduction
c *****
c
imp:n 1 6r 0
```

```
c
c *****
c      Source
c *****
c
sdef sur=888 nrm=-1 erg=d1
spl -2 2.607E-08
```

```
c
c *****
c      Tally
c *****
```

```
c
f4:n 25
c
c *****
c      Material
c *****
c
m1 1001.50 0.66667 6000.50 0.33333
m3 7014.50 0.78457 8016.50 0.21068 18000.35 0.00469 6000.50 0.00006
c
c *****
c      Energy Cards
c *****
c
c
c *****
c      Cutoff Cards
c *****
c
prdmp 3j 1
ctme 720
c ptrac file=asc
c
c *****
c      Peripherals
c *****
c
print
```

APPENDIX B

SAMPLE DATA

The data received from the liquid scintillation counter analyses are given in this appendix. As stated in chapter five, each of the samples were counted in the traditional tritium counting window, channels 0 - 400. A background of 12.84 cpm was automatically subtracted from each sample CPM. Thus, the data given in this appendix is the true counts detected by the liquid scintillation counter.

The DPM expected from the sample at the time of analysis was calculated following the steps outlined in chapter three. The four CPM values obtained from each irradiated sample were averaged.

TRIAL ONE							
<u>sample</u>	<u>mass (g)</u>	<u>CPM</u>	<u>CPM</u>	<u>CPM</u>	<u>CPM</u>	<u>average</u>	<u>statistical error</u>
A-1	0.2008	6220.16	6242.76	6122.16	6116.69	6175.44	28.31
A-2	0.1982	6122.56	6080.56	6082.83	6079.29	6091.31	9.04
A-3	0.2037	6152.76	6112.06	6047.96	6032.03	6086.20	24.36
A-4	0.2009	5992.86	5961.36	5899.63	5873.36	5931.80	23.79
A-5	0.2003	6039.26	5998.36	6025.69	5990.89	6013.55	9.85
A-6	0.2012	6087.66	6043.76	5990.56	5908.29	6007.57	33.42
A-7	0.1996	5982.86	6036.26	6147.56	6101.76	6067.11	31.35
A-8	0.2004	5937.16	5944.46	6354.69	6343.76	6145.02	102.13
A-9	0.2001	6338.76	6314.16	6528.69	6521.36	6425.74	49.85
A-10	0.1996	6255.26	6205.26	6320.29	6321.09	6275.48	24.27
TRIAL TWO							
<u>sample</u>	<u>mass (g)</u>	<u>CPM</u>	<u>CPM</u>	<u>CPM</u>	<u>CPM</u>	<u>average</u>	<u>statistical error</u>
B-1	0.1996	6772.36	6798.89	6180.83	6408.83	6785.63	129.23
B-2	0.2001	6700.56	6668.36	6220.89	6007.23	6684.46	147.63
B-3	0.2013	6865.09	6877.96	6435.03	6207.36	6871.53	143.37
B-4	0.1999	6747.96	6731.36	6351.16	6128.03	6739.66	131.12
B-5	0.2000	6876.29	6837.76	6538.16	6294.49	6857.03	118.49
B-6	0.2021	6747.89	6710.69	6418.09	6139.23	6729.29	123.15
B-7	0.1985	6938.83	6962.43	6577.23	6326.56	6950.63	132.39
B-8	0.1996	6782.89	6815.83	6489.89	6371.29	6799.36	94.73
B-9	0.2000	6807.03	6830.29	6684.56	6123.69	6818.66	143.48

Table B.1: 500 kW Sample Data.

TRIAL ONE							
<u>sample</u>	<u>mass (g)</u>	<u>CPM</u>	<u>CPM</u>	<u>CPM</u>	<u>CPM</u>	<u>average</u>	<u>statistical error</u>
A-1	0.2000	554.99	523.73	535.53	546.86	540.28	5.90
A-2	0.1986	556.89	532.93	557.83	555.39	550.76	5.17
A-3	0.1999	505.49	490.26	508.29	511.96	504.00	4.13
A-4	0.2004	534.83	523.19	546.46	540.03	536.13	4.27
A-5	0.1999	487.83	474.63	501.16	503.39	491.75	5.77
A-6	0.2007	529.86	531.59	542.13	547.06	537.66	3.59
A-7	0.2007	541.03	529.63	568.03	562.89	550.40	7.85
A-8	0.2006	457.16	444.93	474.19	466.19	460.62	5.44
A-9	0.1990	522.06	515.79	538.23	543.19	529.82	5.63
A-10	0.1996	582.49	562.73	585.53	579.99	577.69	4.43
TRIAL TWO							
<u>sample</u>	<u>mass (g)</u>	<u>CPM</u>	<u>CPM</u>	<u>CPM</u>	<u>CPM</u>	<u>average</u>	<u>statistical error</u>
B-1	0.2002	715.13	706.56	701.76	688.76	703.05	4.77
B-2	0.1998	730.33	717.53	697.89	712.49	714.56	5.81
B-3	0.1994	720.89	712.83	700.29	695.46	707.37	5.03
B-4	0.1998	702.99	699.99	698.26	692.26	698.38	1.96
B-5	0.1997	708.56	699.39	689.96	700.83	699.69	3.30
B-6	0.2002	707.93	700.23	694.73	688.63	697.88	3.55
B-7	0.1995	697.26	703.99	691.03	682.23	693.63	4.01
B-8	0.1999	717.66	717.33	708.43	706.76	712.55	2.49
B-9	0.1996	722.93	723.19	707.39	712.06	716.39	3.43

Table B.2: 50 kW Sample Data.

TRIAL ONE							
sample	mass (g)	CPM	CPM	CPM	CPM	average	statistical error
A-1	0.1998	64.29	60.43	65.58	65.39	63.92	1.04
A-2	0.2010	61.86	64.19	65.18	65.28	64.13	0.69
A-3	0.1996	64.09	67.99	63.53	64.43	65.01	0.88
A-4	0.2007	53.43	53.76	62.56	63.91	58.42	2.42
A-5	0.2003	55.26	56.19	60.86	59.63	57.99	1.16
A-6	0.2005	54.99	56.39	60.84	61.89	58.53	1.45
A-7	0.2003	58.59	60.13	61.78	61.01	60.38	0.59
A-8	0.2008	47.13	49.89	50.13	49.73	49.22	0.61
A-9	0.2003	55.53	49.39	55.76	52.94	53.41	1.28
A-10	0.1994	60.16	60.79	63.71	62.94	61.90	0.73
TRIAL TWO							
sample	mass (g)	CPM	CPM	CPM	CPM	average	statistical error
B-1	0.1957	71.84	69.96	65.53	65.74	68.27	1.36
B-2	0.1982	72.74	69.14	67.63	68.76	69.57	0.96
B-3	0.1971	67.41	66.69	67.46	66.66	67.06	0.19
B-4	0.1926	71.74	69.99	69.51	66.06	69.33	1.03
B-5	0.1954	70.98	70.99	66.01	64.38	68.09	1.48
B-6	0.1992	72.79	71.44	66.68	67.14	69.51	1.33
B-7	0.2005	72.48	71.23	68.36	65.76	69.46	1.30
B-8	0.2013	69.59	67.96	66.33	65.91	67.45	0.73
B-9	0.2008	72.81	70.86	66.73	67.94	69.59	1.20

Table B.3: 5 kW Sample Data.

TIME ANALYSIS							
sample	mass (g)	CPM	CPM	CPM	CPM	average	statistical error
A-1	0.2008	5656.96	5651.83	5612.83	5655.03	5644.16	9.09
A-2	0.1982	5374.23	5390.43	5386.96	5368.76	5380.10	4.45
A-3	0.2037	5498.36	5460.89	5442.36	5440.23	5460.46	11.66
A-4	0.2009	5298.43	5285.03	5246.69	5245.69	5268.96	11.63
A-5	0.2003	5362.29	5344.76	5361.96	5313.49	5345.63	9.93
A-6	0.2012	5365.96	5356.96	5330.49	5318.69	5343.03	7.53
A-7	0.1996	5491.69	5504.69	5504.56	5517.29	5504.56	4.53
A-8	0.2004	5542.83	5530.43	5548.36	5513.89	5533.88	6.62
A-9	0.2001	5821.76	5801.43	5773.29	5825.63	5805.53	10.38
A-10	0.1996	5580.96	5538.76	5542.89	5494.76	5539.34	15.27
SOLUTION CONSISTENCY ANALYSIS							
sample	mass (g)	CPM	CPM	CPM	CPM	average	statistical error
A-1	0.2008	5742.23	5670.69	5602.36	5641.23	5664.13	25.60
A-2	0.1982	5475.56	5391.76	5352.49	5383.56	5400.84	22.78
A-3	0.2037	5888.63	5806.56	5770.03	5824.83	5822.51	21.49
A-4	0.2009	5779.29	5659.89	5659.23	5684.49	5695.73	24.65
A-5	0.2003	5758.69	5707.43	5662.56	5682.56	5702.81	17.98
A-6	0.2012	5911.16	5745.03	5745.23	5730.23	5782.91	37.15
A-7	0.1996	5683.29	5571.63	5547.49	5572.43	5593.71	26.34
A-8	0.2004	5793.29	5745.09	5673.23	5712.09	5730.93	22.04
A-9	0.2001	6388.03	6279.43	6242.63	6231.23	6285.33	30.96
A-10	0.1996	5798.56	5686.96	5676.36	5669.43	5707.83	26.38

Table B.4: Time And Consistency Sample Data.

M97053619



Report Number (14) DOE/OR/00033 -- T742

Publ. Date (11) 1996
Sponsor Code (18) DOE/EH, XF
UC Category (19) UC-600, DOE/ER

DOE